1-1-2009

Darriwilian (Middle Ordovician) conodonts from Thompson Creek, Nelson Province, New Zealand

Yong Yi Zhen
Australian Museum

Ian G. Percival
Geological Survey of New South Wales, ian.percival@industry.nsw.gov.au

Roger A. Cooper
Institute of Geological and Nuclear Sciences

John E. Simes
Institute of Geological and Nuclear Sciences

Anthony J. Wright
University of Wollongong, awright@uow.edu.au

Darriwilian (Middle Ordovician) conodonts from Thompson Creek, Nelson Province, New Zealand

Abstract

A well preserved Middle Ordovician conodont fauna of 24 species has been recovered from seven samples of a small limestone lens exposed in Thompson Creek, northwest of Nelson, on the South Island of New Zealand. The presence of Histiodella holodentata, Baltoniodus? sp., Paroistodus originalis, P. horridus, Periodon macrodentatus, Protopanderodus sp. cf. P. varicostatus, Costiconus ethingtoni and Venoistodus balticus in the fauna indicates a Darriwilian (late Da2 to mid Da3) age. The occurrence of Ansella jemtlandica, Baltoniodus? sp., Periodon macrodentatus, Spinodus sp., Spinodus? sp. and Histiodella holodentata suggests a relatively deeper water (outer shelf to slope) setting, comparable with contemporaneous faunas, in the lower part of the Weemalla Formation and from allochthonous limestones within the Oakdale Formation of central New South Wales.

Keywords

Conodonts, Middle Ordovician, Darriwilian, Thompson Creek, New Zealand, biostratigraphy, GeoQUEST

Disciplines

Life Sciences | Physical Sciences and Mathematics | Social and Behavioral Sciences

Publication Details

Zhen, Y., Percival, I. G., Cooper, R. A., Simes, J. E. & Wright, A. J. (2009). Darriwilian (Middle Ordovician) conodonts from Thompson Creek, Nelson Province, New Zealand. Memoirs of the Association of Australasian Palaeontologists, 37 25-53.

Darriwilian (Middle Ordovician) conodonts from Thompson Creek, Nelson Province, New Zealand

YONG YI ZHEN, IAN G. PERCIVAL, ROGER A. COOPER, JOHN E. SIMES & ANTHONY J. WRIGHT

ZHEN, Y.Y., PERCIVAL, I.G., COOPER, R.A., SIMES, J.E. & WRIGHT, A.J., 2009:12:24. Darriwilian (Middle Ordovician) conodonts from Thompson Creek, Nelson Province, New Zealand. *Memoirs of the Association of Australasian Palaeontologists 37*, 25-53. ISSN 0810-8889.

A well preserved Middle Ordovician conodont fauna of 24 species has been recovered from seven samples of a small limestone lens exposed in Thompson Creek, northwest of Nelson, on the South Island of New Zealand. The presence of *Histiodella holodentata*, *Baltoniodus*? sp., *Paroistodus originalis*, *P. horridus*, *Periodon macrodentatus*, *Protopanderodus* sp. cf. *P. varicostatus*, *Costiconus ethingtoni* and *Venoistodus balticus* in the fauna indicates a Darriwilian (late Da2 to mid Da3) age. The occurrence of *Ansella jemtlandica*, *Baltoniodus*? sp., *Periodon macrodentatus*, *Spinodus* sp., *Spinodus*? sp. and *Histiodella holodentata* suggests a relatively deeper water (outer shelf to slope) setting, comparable with contemporaneous faunas, in the lower part of the Weemalla Formation and from allochthonous limestones within the Oakdale Formation of central New South Wales.

Yong Yi Zhen (yongyi.zhen@austmus.gov.au), Palaeontology Section, Australian Museum, 6 College St, Sydney NSW 2010, Australia; Ian G. Percival (ian.percival@dpi.nsw.gov.au), Geological Survey of New South Wales, Department of Primary Industries, W.B. Clarke Geoscience Centre, 947-953 Londonderry Road, Londonderry NSW 2753, Australia; Roger A. Cooper (r.cooper@gns.cri.nz) and John E. Simes (j.simes@gns.cri.nz), Institute of Geological and Nuclear Sciences, P.O. Box 30 368, Lower Hutt, New Zealand; Anthony J. Wright (tony_wright@uow.edu.au), School of Earth and Environmental Sciences, University of Wollongong, Wollongong, NSW 2522, Australia. *Received 6 March 2009.*

Keywords: Conodonts, Middle Ordovician, Darriwilian, Thompson Creek, New Zealand, biostratigraphy.

ORDOVICIAN faunas from carbonate horizons and isolated blocks are relatively rare in New Zealand, and are confined to the Takaka Terrane of Nelson Province, in the northwest of New Zealand's South Island (Fig. 1). Wright (1968) first reported Middle Ordovician conodonts in the area, and Simes (1980) recorded latest Darriwilian to earliest Gisbornian (Sandbian) conodonts from the lower part of the Arthur Marble at Mount Owen. Conodonts from the Summit Limestone of Early Ordovician (Tremadocian) age at Mount Patriarch were documented by Cooper & Druce (1975), and a latest Cambrian to earliest Ordovician conodont and trilobite fauna was described from the underlying Patriarch Formation (Wright *et al*. 1994). In the adjacent Buller Terrane, deeper water siltstones contain an extensive graptolite sequence at Aorangi Mine (Cooper 1979), and have also yielded the trinucleid trilobite *Incaia* from Gisbornian (Sandbian, early Late Ordovician) strata on the Paturau River (Hughes & Wright 1970). Given these sparse records, any additional occurrences which enable increased biostratigraphic precision, are of considerable significance. Here we describe a diverse conodont fauna of mid-Darriwilian age that helps constrain models of Takaka Terrane biostratigraphy.

SAMPLING AND GEOLOGICAL SETTING

The fossils described here were recovered from seven spot samples (Table 1) collected from a small limestone lens, approximately 25 m thick that outcrops in the true left branch of Thompson Creek, 150 m upstream from its junction with the true right branch, and 1.5 km upstream from the confluence with the Paturau River, at grid reference M25/676582 (Fig.1). The lens was found by D.G. Bishop (Bishop 1965) who noted

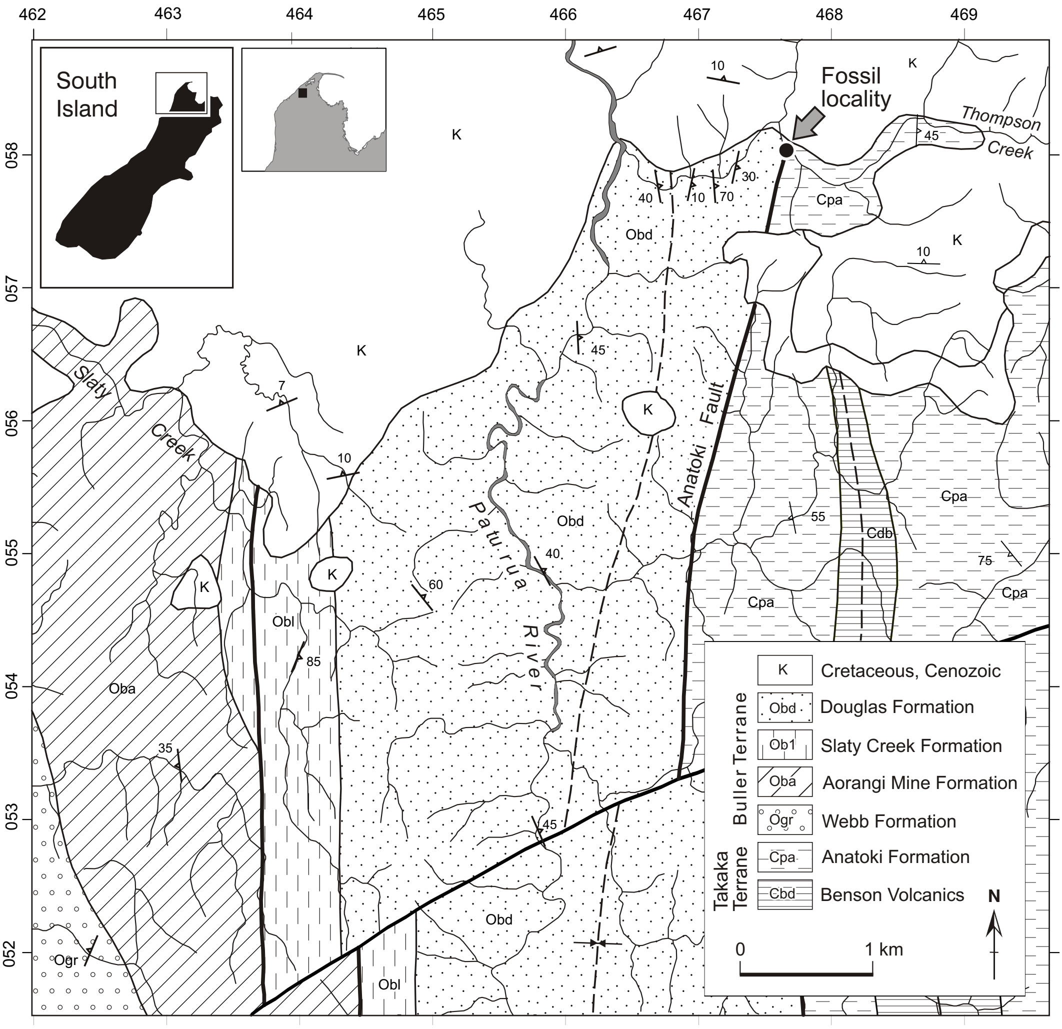

Fig. 1. Locality map of the study area in Nelson Province, South Island, New Zealand, showing terrane boundaries and localities mentioned in text.

'comminuted shell fragments', and who later mapped it as ?Arthur Marble (Bishop 1971). The presence of Middle Ordovician conodonts in the lens was reported by Wright (1968).

Stratigraphic contacts are not exposed. The Thompson Creek lens is interpreted as an allochthonous block within a broad zone of major transcurrent and thrust faulting, the Anatoki Fault, and is therefore inferred to be fault bounded. The Anatoki Fault separates the Buller Terrane from the Takaka Terrane. To the west, in Thompson Creek and the Paturau River, dark shale, quartz sandstone and green laminated siltstone are mapped as Douglas Formation (Golden Bay Group, Buller Terrane) by Rattenbury *et al*. (1998). Graptolites from this unit indicate an age range from late Darriwilian to Gisbornian, and include dicellograptid fragments in Thompson Creek, and *Nemagraptus gracilis* and *Dicranograptus nicholsoni* in Paturau River (Cooper 1979). To the east lies Late Cambrian siliceous and volcanogenic green sandstone, mapped by Bishop (1971) and Rattenbury *et al*. (1998) as Anatoki Formation (Mount Patriarch Group, Takaka Terrane). From its age and lithology, the Thompson Creek lens is interpreted as equivalent to the uppermost part of the Summit Limestone of Rattenbury *et al*. (1998), part of the Takaka Terrane succession.

To the south, in the Cobb Valley and Mount Patriarch areas, the Summit Limestone contains conodonts which indicate an age range of latest Cambrian to Middle Ordovician (Darriwilian: Cooper & Bradshaw 1986, Cooper 1989). Darriwilian conodonts from the uppermost beds of the Arthur Marble, the stratigraphic equivalent of

Conodont species \ Samples	CN640	CN641	CN642	CN917	CN918	1-39	CN-1076	Total
Ansella jemtlandica	2	10	7			9	1	**29**
Baltoniodus? sp.	2		1			1		**4**
Cornuodus longibasis		1				2		**3**
Costiconus ethingtoni		35						**35**
Costiconus sp. cf. *C. iniquus*		11						**11**
Drepanodus sp. cf. *D. reclinatus*	4	52	17			4		**77**
Drepanoistodus costatus		42						**42**
Drepanoistodus tablepointensis	5	42						**47**
Gen. et sp. indet.	1	9		1		1		**12**
Histiodella holodentata						1		**1**
Microzarkodina sp.		1				1		**2**
Oistodus sp. cf. *O. lanceolatus*	91	65	13			4		**173**
Parapaltodus simplicissimus	1							**1**
Paroistodus horridus					21		5	**26**
Paroistodus originalis	7	88	4	2		4	1	**106**
Periodon macrodentatus	11	90	59		16	19	4	**199**
Protopanderodus cooperi		4						**4**
Protopanderodus? *nogamii*	2	13			3	1		**19**
Protopanderodus rectus	1							**1**
Protopanderodus sp. cf. *P. varicostatus*	25	76		2	2	2		**107**
Spinodus sp.	2	7		1			1	**11**
Spinodus? sp.		1						**1**
Triangulodus sp.	10	24	8			1		**43**
Venoistodus balticus	2							**2**
Total	**166**	**571**	**109**	**6**	**42**	**50**	**12**	**956**

Table 1. Distribution of conodont species in the samples studied.

the Summit Limestone in the Eastern Sedimentary Belt of the Takaka Terrane, were described by Simes (1980).

AGE AND CORRELATION

Middle Ordovician conodonts from Thompson Creek in Nelson Province were first reported by Wright (1968) who suggested a Llanvirnian age on the basis of a limited and undescribed fauna. *Pygodus anserinus*, a distinctive index zonal species ranging across the Middle/Late Ordovician boundary was recorded with several other conodonts from nearby Mount Owen (Simes 1980).

Twenty-four conodont species are distinguished in the fauna from Thompson Creek (Table 1). Age-diagnostic species described herein include *Histiodella holodentata*, *Baltoniodus*? sp., *Paroistodus originalis*, *P. horridus*, *Periodon macrodentatus*, *Protopanderodus* sp. cf. *P. varicostatus*, *Costiconus ethingtoni* and *Venoistodus balticus*. This conodont fauna indicates a middle Darriwilian (late Da2 to mid Da3) age, comparable with contemporaneous faunas from the lower part of the Weemalla Formation and from allochthonous limestones within the Oakdale Formation in central New South Wales (Zhen & Percival 2004a, b).

Species of *Histiodella* are especially important in fine-scale biozonation and worldwide correlation of lower to middle Darriwilian strata. In Middle Ordovician shallow water successions of the North American Mid-Continent region, three conodont zones – in ascending order, *H. altifrons*, *H. sinuosa* and *H. holodentata* zones – were recognised in Utah by Ethington & Clark (1982; also see Sweet 1988; Pyle *et al*. 2003). Three species of *Histiodella* occur in the lower and middle members of the Table Head Formation in western Newfoundland, providing the basis for establishment of two conodont biozones (Stouge 1984): the *H. tableheadensis* Zone in the lower-middle part of the lower member, succeeded by the *H. kristinae* Zone from the upper part of the lower member to the top of the middle member. The third species, *H. bellburnensis*, is restricted to the top part of the *H. kristinae* Zone. The oldest of Stouge's three species, *H. tableheadensis*, is now considered to be a junior synonym of *H. holodentata*, which has been widely reported in North America, Scandinavia, Poland, Estonia, China and Australia. In the Table Head Formation, *H. holodentata* ranges through the entire lower member (Stouge 1984, fig. 18), and the *H. holodentata* Zone (= *H. tableheadensis* Phylozone) was correlated to the mid-upper *variabilis* Zone of Scandinavian successions (see Stouge, 1984, table 3). Chen *et al*. (2006) correlated the base of the *H. holodentata* Zone in western Newfoundland with the lower part of the *A. ellesae* graptolite Zone of late Da2 age. In the Ibex area of Utah, the *H. holodentata*

Zone was also correlated with the *variabilis* Zone (approximately equivalent to Da2, see Webby *et al*. 2004) in Scandinavia (Ethington & Clark 1982; Sweet 1988). However, Pyle *et al*. (2003) considered the *H. altifrons* Zone as basal Darriwilian (Da1) in age, and correlated the *H. holodentata* Zone with the middle Darriwilian (approximately equivalent to Da3).

A comparable zonal succession was established by Du *et al*. (2005) for the early-mid Darriwilian in the Tarim Basin of western China, characterised by four species of *Histiodella* (in ascending order): *H. sinuosa* Zone, *H. holodentata* Zone, *H. kristinae* Zone, and *H. bellburnensis* Zone. Du *et al*. (2005) suggested correlation of their *H. kristinae* Zone with the upper *variabilis* and lower *suecicus* zones of the Scandinavian successions (approximately equivalent to late Da2 to early Da3). This was more or less in agreement with Stouge (1984), who correlated the *H. kristinae* Zone with the *suecicus* Zone (of Da3 age). In eastern Australia, *H. holodentata* (identified as *H. kristinae*) has been recorded from allochthonous limestone blocks (assigned an early-mid Da3 age) within the Oakdale Formation of central New South Wales (Zhen & Percival 2004a). Recent study of the upper Darriwilian section at Huangnitang, Zhejiang Province in South China by Chen *et al*. (2006) enabled precise correlation between conodont and graptolite zonations. Both the *H. holodentata* and *H. kristinae* zones were recognised in the Hulo Formation, with the former correlated with the *N. fasciculatus* graptolite Zone of mid Da3 age, and the latter with the lower *P. elegans* graptolite Zone of late Da3 age (Chen *et al*. 2006, figs 12, 13). This correlation implies a slightly younger base for the *H. holodentata* Zone defined in the Hulo Formation of South China than was recognised in western Newfoundland, but accords well with the correlation of Pyle *et al*. (2003) in Alberta.

Paroistodus horridus ranges from the middle *variabilis* Zone to middle *suecicus* Zone (approximately equivalent to Da2-3) in the middle member of the Gualcamayo Formation of the Argentine Precordillera (Albanesi & Barnes 2000, fig. 2). A similar stratigraphic range for *P. horridus* was also recorded in the Table Head Formation of western Newfoundland, ranging through the mid-upper *H. holodentata* Zone to *H. kristinae* Zone (see Stouge 1984, fig. 18). However, Löfgren (1995) reported the occurrence of *P.* sp. aff. *horridus* from considerably older strata (upper Floian, upper *O. evae* Zone) in Sweden.

Although *P. horridus* and *H. holodentata* are relatively rare in Thompson Creek samples, with *H. holodentata* represented by only one specimen (from sample 1-39), and *P. horridus* represented by 26 specimens from two samples (CN918 and CN1076, see Table 1), their co-occurrence suggests a mid Darriwilian age (late Da2 to mid Da3), comparable with the fauna from allochthonous limestone blocks in the Oakdale Formation of central New South Wales (Zhen & Percival 2004a). Relatively abundant *Periodon macrodentatus*, *Paroistodus originalis* and *Protopanderodus* cf. *varicostatus* in other Thompson Creek samples confirm this generalised mid Darriwilian age.

The common appearance of *Paroistodus originalis* tends to imply a slightly older age; Albanesi & Barnes (2000, fig. 4) indicated that *P. originalis* might be the direct ancestor of *P. horridus* with a minimum Da2 age (middle *variabilis* Zone). In the Potrerillo Mountain section of the Argentine Precordillera, the youngest *P. originalis* and oldest *P. horridus horridus* were found co-occurring only in one sample at the very base of the middle member of the Gualcamayo Formation. Albanesi (in Albanesi *et al*. 1998) further proposed two subspecies of *P. horridus* (*P. horridus secundus* and *P. horridus primus*) representing primitive forms of the species, which were recorded at the top of the lower member of the Gualcamayo Formation in association with *P. originalis*. Unfortunately, specimens assigned to *P. horridus* from Thompson Creek are too poorly preserved for determination of subspecies. However, the association of *P. originalis*, *P. horridus* and rare *H. holodentata* in this fauna enables us to constrain its age in a range from late Da2 to mid Da3.

SYSTEMATIC PALAEONTOLOGY (Zhen)

All illustrations in Figures 2 to 11 are SEM photomicrographs. The 122 figured specimens bearing the prefix CNP (CNP1081 – CNP1202) are deposited in the New Zealand Institute of Geological and Nuclear Sciences, Lower Hutt. Sample localities are shown in Fig. 1; and details of these sites are provided above. Numbers with prefix IY are SEM digital image filenames. The conodont species *Cornuodus longibasis* (Lindström, 1955), *Parapaltodus simplicissimus* Stouge, 1984, and *Protopanderodus rectus* (Lindström, 1955) are rare and documented by illustration only.

Phylum CHORDATA Balfour, 1880
Class CONODONTA Pander, 1856

Ansella Fåhræus & Hunter, 1985

Type species. *Belodella jemtlandica* Löfgren, 1978.

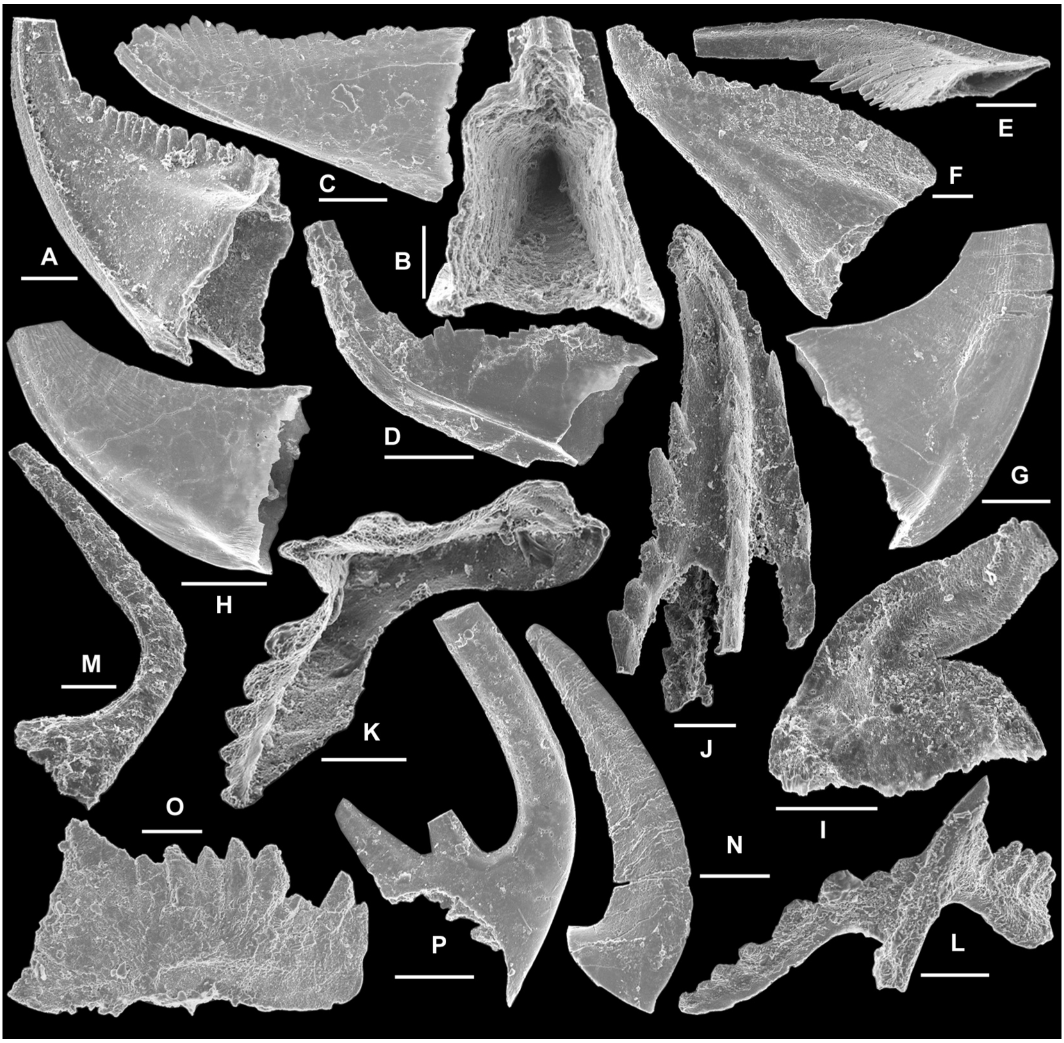

Fig. 2. **A-I**, *Ansella jemtlandica* (Löfgren, 1978). **A, B**, Sa element, CNP1081, CN642, **A**, lateral view (IY100-10); **B**, basal view (IY100-09). **C**, Sb element, CNP1082, CN641, inner lateral view (IY93-42). **D**, Sb element, CNP1083, CN641, outer lateral view (IY93-41). **E**, Sc element, CNP1084, CN640, postero-basal view (IY99-34). **F**, Sc element, CNP1085, CN642, outer lateral view (IY100-08). **G**, Pb element, CNP1086, CN641, outer lateral view (IY94-01). **H**, Pb element, CNP1087, CN641, inner lateral view (IY93-43). **I**, M element, CNP1088, CN917, posterior view (IY109-041). **J-L**, *Baltoniodus*? sp. **J**, Sd element, CNP1089, CN642, postero-lateral view (IY100-13). **K-L**, Pa element, CNP1090, 1-39, **K**, basal view (IY101-07); **L**, anterior view (IY101-06). **M**, *Cornuodus longibasis* (Lindström, 1955). Sc element, CNP1091, 1-39, outer lateral view (IY101-08). **N**, *Parapaltodus simplicissimus* Stouge, 1984. CNP1092, CN641, lateral view (IY101-27). **O**, *Histiodella holodentata* Ethington & Clark, 1982. Pa element, CNP1093, 1-39, outer lateral view (IY100-14). **P**, *Spinodus*? sp. S element, CNP1094, CN641, inner lateral view (IY93-40). Scale bars 100 µm.

Ansella jemtlandica (Löfgren, 1978) (Fig. 2A-I)

1978 *Belodella jemtlandica*; Löfgren, p. 46, pl. 15, figs 1-8, fig. 24A-D.
2004a *Ansella jemtlandica* (Löfgren); Zhen & Percival, p. 84-86, fig. 5A-Q (cum syn.).
2004b *Ansella jemtlandica* (Löfgren); Zhen & Percival, fig. 4A-G.

Material. 29 specimens from five samples (see Table 1).

Remarks. Five element types including adenticulate makellate M (Fig. 2I), Pb element (Fig. 2G-H), symmetrical bicostate Sa (Fig.

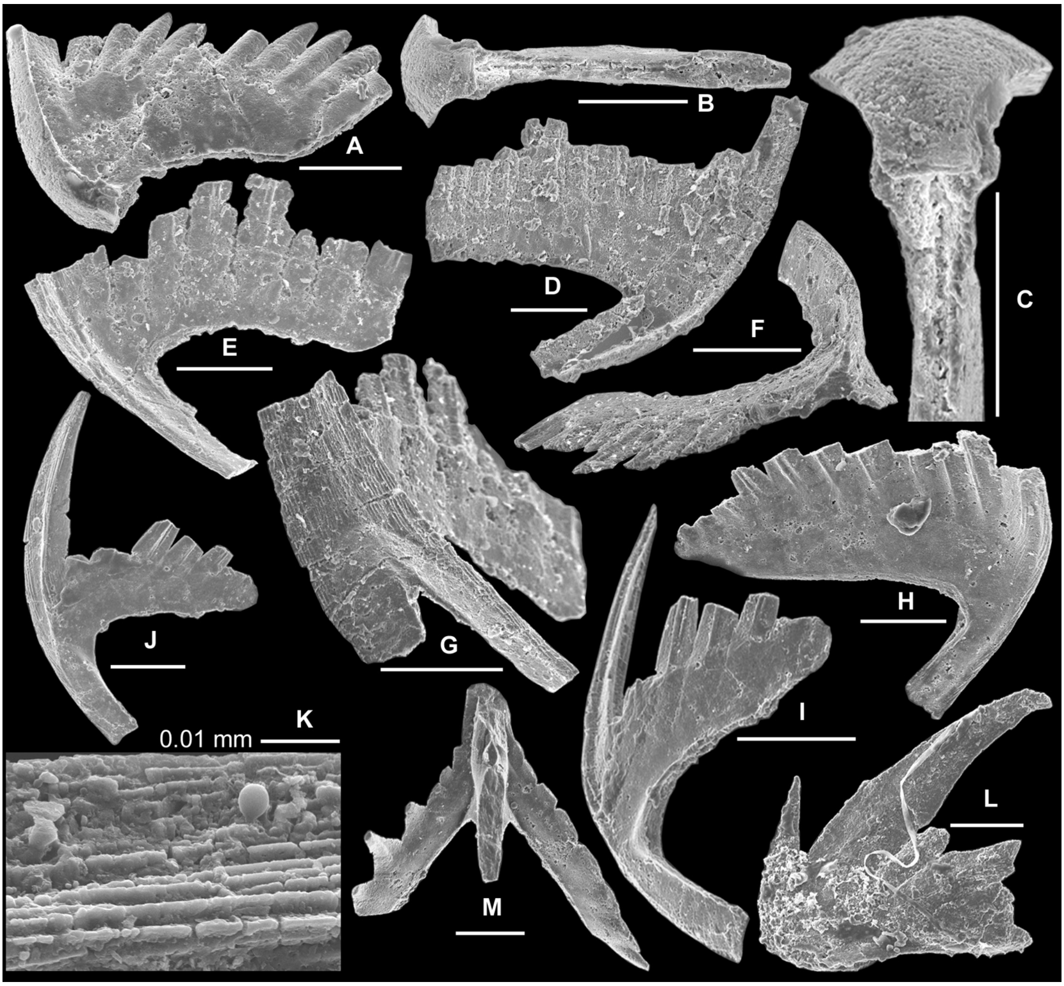

Fig. 3. **A-C**, *Baltoniodus*? sp. Sa element, CNP1095, CN641; **A**, lateral view (IY109-17), **B**, basal view (IY109-16), **C**, basal view, close up showing basal cavity and broad anterior face (IY109-16). **D-K**, Gen. et sp. indet. **D**, Sa element, CNP1096, 1-39, lateral view (IY109-44). **E-G**, Sb element, CNP1097, CN640, **E**, outer lateral view (IY108-33), **F**, upper view (IY108-35), **G**, antero-outer lateral view (IY108-34). **H**, Sc element, CNP1098, CN641, inner lateral view (IY109-18). **I-K**, Sd element, CNP1099, CN641, **I**, basal-outer lateral view (IY96-05), **J**, outer lateral view (IY96-03), **K**, outer lateral view, close up showing surface striae (IY96-04). **L-M**, *Microzarkodina* sp. **L**, P element, CNP1100, 1-39, inner lateral view (IY100-15); **M**, Sb element, CNP1101, CN641, posterior view (IY107-018). Scale bars 100 µm, unless otherwise indicated.

2A-B), asymmetrical bicostate Sb (Fig. 2C-D), and acostate Sc (Fig. 2E-F) were recovered. They compare well with those from Darriwilian faunas from allochthonous blocks in the Oakdale Formation (Zhen & Percival 2004a) and from limestones in the lower Weemalla Formation (Zhen & Percival 2004b) of New South Wales.

Baltoniodus Lindström, 1971

Type species. *Prioniodus navis* Lindström, 1955.

Baltoniodus? sp. (Figs 2J-L, 3A-C)

Material. Four specimens representing Pa, Sa and Sd elements (see Table 1).

Description. Pa element pastinate (Fig. 2K-L) with a long denticulate posterior process, a short denticulate anterior process and a long denticulate outer lateral process; cusp robust with sharp anterior and posterior margins, and a sharp costa on the outer lateral face; outer lateral process extending anterolaterally with a wide angle (more than 90°) between the outer lateral and posterior processes; anterior process with only two or three small denticles distally; basal cavity open and moderately deep.

Sa element alate (Fig. 3A-C), with a long denticulate posterior process; cusp prominent, suberect, triangular in cross section with a wide, rounded anterior face, a posterior costa and a blade-like costa on each side; denticles on the posterior process regular in size, closely spaced with confluent bases and pointed tips, and posteriorly reclined; basal cavity small, extending posteriorly as a narrow and shallow groove.

Sd element quadriramate (Fig. 2J), weakly asymmetrical, with a denticulate posterior process, an inwardly curved anterior process with small or rudimentary denticles along its upper edge, and a denticulated lateral process on each side.

Remarks. The four specimens available are treated as a single taxon, but they may represent different species or even genera of Prioniodontidae. As the denticulation, especially on the posterior process of the S elements, differs significantly from that of typical *Baltoniodus*, these specimens are only doubtfully assigned to that genus. The two Pa elements resemble those of *B. medius* from Jämtland, northern Sweden, described in detail by Löfgren (1978). However, the Sa element (Fig. 3A-C) has a longer posterior process which bears regular-sized and reclined denticles, and the Sd element (Fig. 2J) has weaker development of denticles, in particular on the anterior process.

Costiconus Rasmussen, 2001

Type species. Panderodus ethingtoni Fåhraeus, 1966.

Remarks. The type species of *Walliserodus* Serpagli, 1967, *Acodus curvatus* Branson & Branson, 1947, is Silurian. Fåhraeus & Hunter (1985, p. 1179) indicated that the Silurian and Ordovician forms previously included in *Walliserodus* by various authors differed considerably in their proposed compositions and likely represented separate natural groups. Following this notion, Rasmussen (2001) proposed *Costiconus* with *Panderodus ethingtoni* Fåhraeus, 1966 as the type species, to accommodate those Ordovician forms previously referred to *Walliserodus*. *Costiconus* was defined as having a trimembrate apparatus including drepanodiform (=P elements herein), oistodiform (=M element herein) and costate elements (=S elements herein). *Costiconus* differs from *Protopanderodus* in having a deeper basal cavity and thinner wall without the posterior extension of the base.

Costiconus ethingtoni (Fåhraeus, 1966) (Fig. 4H-W)

1966 *Panderodus ethingtoni*; Fåhraeus, p. 26, pl. 3, fig. 5a-b.
1974 *Walliserodus ethingtoni* (Fåhraeus); Bergström *et al*., pl. 1, fig. 12.
1978 *Walliserodus ethingtoni* (Fåhraeus); Löfgren, p. 114-116, pl. 4, figs 27-35, text-fig. 33 (cum syn.).
1985 *Walliserodus ethingtoni* (Fåhraeus); Fåhraeus & Hunter, p. 1180, pl. 3, figs 11-16, text-fig. 6.
1987 *Walliserodus ethingtoni* (Fåhraeus); An, p. 195-196, pl. 8, figs 28-31, pl. 12, fig. 22.
1998 *Walliserodus ethingtoni* (Fåhraeus); Zhang, p. 95-96, pl. 18, figs 10, 12-15, ?11 (cum. syn.).
1998 *Walliserodus ethingtoni* (Fåhraeus); Albanesi *et al*., p. 115, pl. 14, figs 20-25, text-fig. 8.
2000 *Walliserodus ethingtoni* (Fåhraeus); Zhao *et al*., p. 230, pl. 22, figs 1-6.
2001 *Costiconus ethingtoni* (Fåhraeus); Rasmussen, p. 62-64, pl. 3, figs 16-18 (cum syn.).

Material. 35 specimens from sample CN641.

Remarks. Löfgren (1978) documented in detail a wide variation of the S elements in respect to the number of costae of this species, based on a large collection from the Middle Ordovician (Darriwilian) in Sweden, and recognised 17 different morphotypes with the number of the costa varying from two to eleven (see Löfgren 1978, text-fig. 33). Fåhraeus & Hunter (1985) proposed a species apparatus consisting of eight elements including symmetrical and asymmetrical multicostate, and acostate (scandodiform) elements. This latter interpretation has been accepted by most subsequent workers (Zhang 1998; Albanesi *et al*. 1998). Zhang (1998, pl. 18, fig. 11) also recognised a scandodiform M element in the species, but this assignment is here considered doubtful. Rasmussen (2001) defined *Costiconus ethingtoni* Fåhraeus, 1966 as having a trimembrate apparatus including drepanodiform (=P element), oistodiform (=M element) and costate elements (=S elements), with the latter forming a symmetry-transition series of more than 19 different variations based on the location and number of costae on the lateral faces. Previous authors (e.g., Löfgren 1978; Rasmussen 2001) have shown that the number and location of the costae on the lateral faces of the S elements are not the only characters on which to differentiate various morphotypes of the

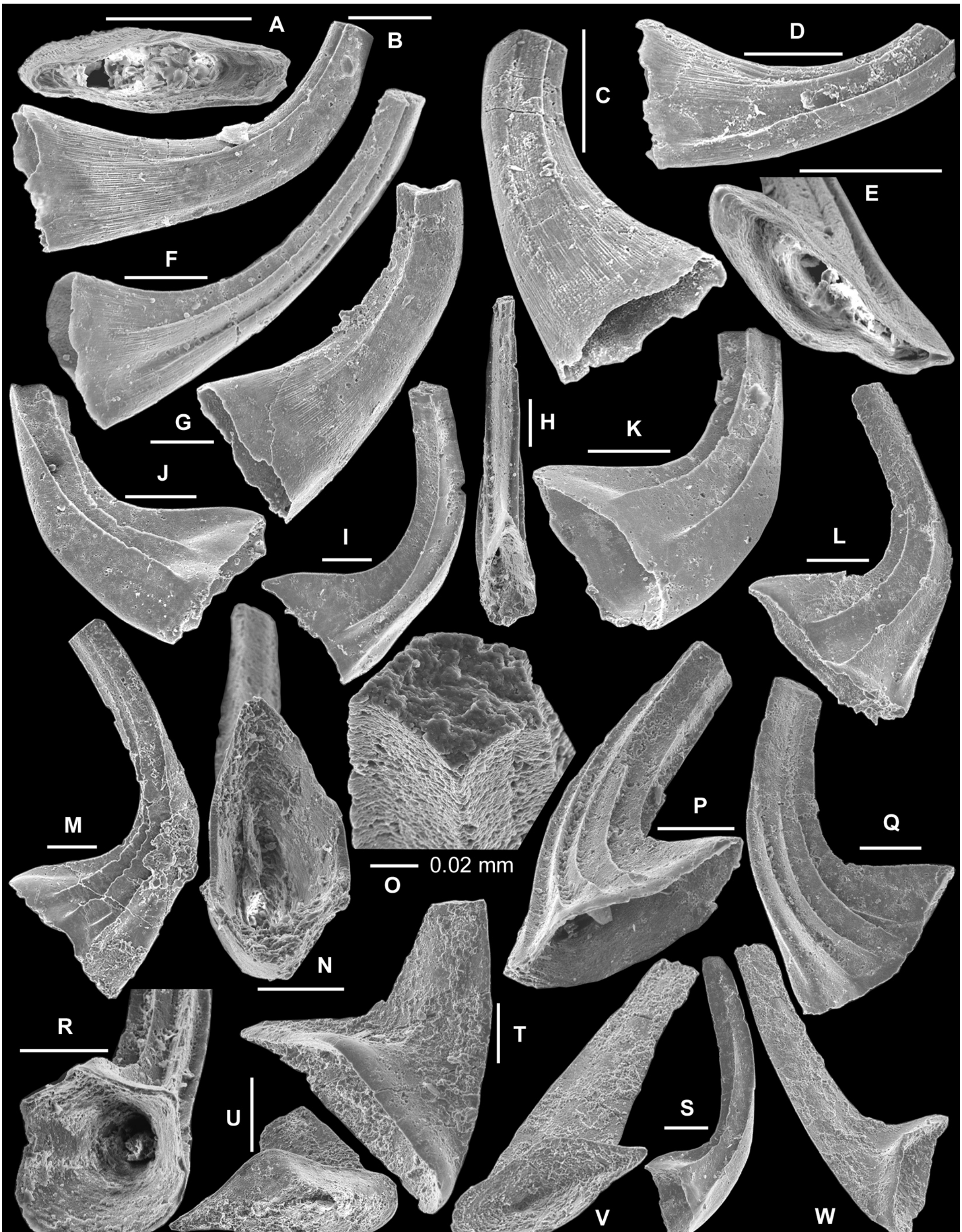

Fig. 4. **A-G**, *Costiconus* sp. cf. *C. iniquus* (Viira, 1974). **A-B**, Sa element, CNP1102, **A**, basal view (IY109-31), **B**, lateral view (IY109-30). **C-D**, Sb element, CNP1103, **C**, outer lateral view (IY109-32), **D**, inner lateral view (IY109-34). **E-G**, Sc element, CNP1104, **E**, oblique basal view (IY109-28), **F**, inner lateral view (IY109-29); **G**, CNP1105, outer lateral view (IY109-25). **H-W**, *Costiconus ethingtoni* (Fåhraeus, 1966); **H-I**, Sa element, CNP1106, **H**, postero-basal view (IY100-19); **I**, lateral view (IY100-20); **J-K**, Sa element, CNP1107, lateral views (IY100-21, IY100-24). **L-N**, Sb element; **L**, CNP1108, inner lateral view (IY100-26); **M-N**, CNP1109, **M**, outer lateral view (IY100-29), **N**, basal view (IY100-28). **O-Q**, Sc element, CNP1110, **O**, upper view close up showing cross section of the cusp (IY100-30), **P**, basal-outer lateral view (IY100-32), (*continued opposite)*

S elements. Rasmussen's definition is followed herein, but only drepanodiform P (Fig. 4T-W), and costate S elements are represented in the material from Thompson Creek. The outline of the base, combined with the number and location of costae on the lateral faces, is employed herein to differentiate four major types of S elements. The Sa element (Fig. 4H-K) is symmetrical, laterally compressed, with an oval outline of the base, and typically with two costae on each side. The Sb element (Fig. 4L-N) also has an oval outline of the base, but is asymmetrical, and the costae on the lateral faces vary considerably in number and position. The Sc element (Fig. 4O-Q) is most strongly laterally compressed and typically multicostate. The Sd element (Fig. 4R-S) is nearly symmetrical, and the outline of the base is typically pentagonal and the base is least laterally compressed. Concurrent with Rasmussen's (2001) definition of *Costiconus*, Zhang & Barnes (2002) revised *Walliserodus* and its type species, *W. curvatus*, based on a large collection from the Llandovery of Anticosti Island, Québec. They suggested a quinquimembrate apparatus for *Walliserodus*, including unicostatiform (=P element), dyscritiform (=Sa), deboltiform (=Sb), curvatiform (=Sc), and multicostatiform (=Sd) elements. Their revised *Walliserodus* includes not only Silurian species, but also Late Ordovician species such as *W. amplissimus* (Serpagli), unlike Rasmussen (2001) who proposed splitting Ordovician forms from *Walliserodus* to establish *Costiconus*. Although neither Rasmussen (2001) nor Zhang & Barnes (2002) made a detailed comparison of the types of *C. ethingtoni* and *W. curvatus*, such a study is well beyond the scope of the current contribution, and therefore *Costiconus* is tentatively considered as a valid genus.

Costiconus sp. cf. C. iniquus (Viira, 1974) (Fig. 4A-G)

cf. 1974 *Paltodus iniquus*; Viira, p. 99, pl. 11, figs 16-17.
cf. 1978 *Walliserodus iniquus* (Viira); Löfgren, p. 116-117, pl. 4, figs 15-26 (cum syn.).

Material. 11 specimens (representing Sa, Sb and Sc elements) from sample CN641.

Description. Costate coniform elements with a proclined cusp and a base of moderate depth; costae not reaching the basal margin; surface ornamented with fine striae. Sa element symmetrical, laterally compressed with a long base; cusp with a broad anterior face, and a sharp costa on each side located more towards posterior margin. Sb element like Sa, but asymmetrical with two stronger costae on the inner lateral face and two weaker costae on the outer lateral face. Sc element strongly compressed laterally and asymmetrical with a shorter base, and with two strong costae on the inner face and one weaker costa on the outer lateral face.

Remarks. The morphology of the current material is comparable with *C. iniquus* from the Darriwilian of northern Sweden (Löfgren 1978), except that the number and position of the costae do not match that of the Swedish material. Löfgren (1978) recognised three morphotypes referred to as A, B and C types for *C. iniquus*. Type A (=Sa element) is symmetrical with two costae on each side; type B (=Sb element) is weakly asymmetrical with two costae on the outer lateral face and one costa on the inner lateral face; and type C is strongly asymmetrical and variable in the number of costae, typically with one or two costae on the outer lateral side and one to three costae on the inner side.

Drepanodus Pander, 1856

Type species. *Drepanodus arcuatus* Pander, 1856.

Drepanodus sp. cf. D. reclinatus (Lindström, 1955) (Fig. 5A-R)

cf. 1955 *Acontiodus reclinatus*; Lindström, p. 548, text-fig. 3C, pl. 2, figs 5-6.
cf. 2003 *Drepanodus reclinatus* (Lindström); Löfgren & Tolmacheva, p. 216-217, figs 5A-J, 7A-G (cum syn.).

Material. 77 specimens from four samples (see Table 1).

Description. Large hyaline elements. S elements with a long base and a costate cusp; Sa element symmetrical, cusp suberect and laterally compressed with a sharp anterior margin, a sharply costate posterior margin and a sharp posterolateral costa on each side (Fig. 5A-B); base pyriform in outline (Fig. 5A). Sb element (Fig. 5C-F) asymmetrical, with a suberect or distally

Q, outer lateral view (IY100-31). **R-S**, Sd element, CNP1111, **R**, basal view, close up showing outline of the base (IY100-18), **S**, lateral view (IY100-17). **T-W**, P element; **T-U**, CNP1112, **T**, inner lateral view (IY94-29), **U**, IY94-28); **V-W**, CNP1113, **V**, basal view (IY94-28), **W**, inner lateral view (IY94-27). All from CN641; scale bars 100 μm, unless otherwise indicated.

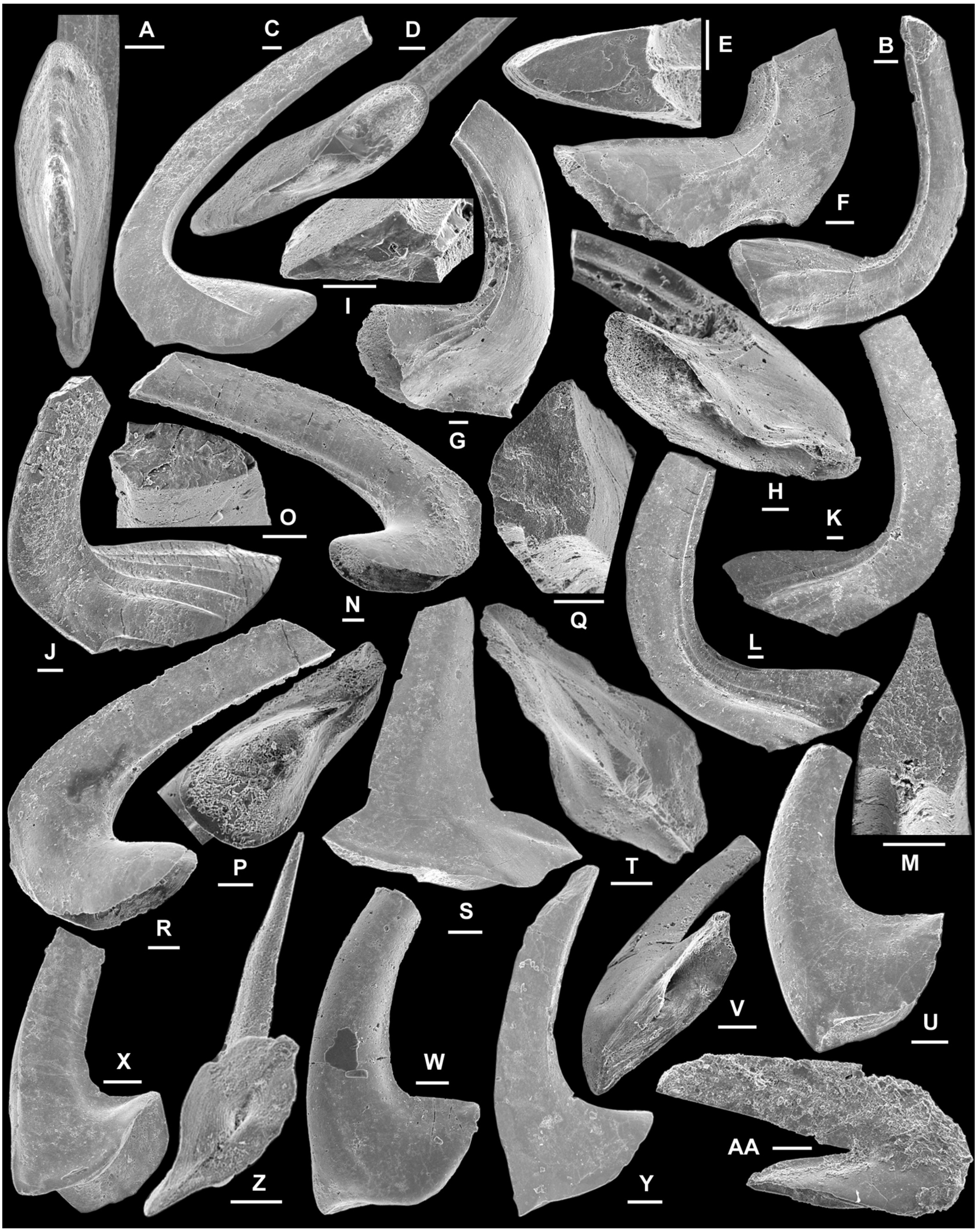

Fig. 5. **A-R**, *Drepanodus* sp. cf. *D. reclinatus* (Lindström, 1955). **A-B**, Sa element; **A**, CNP1114, CN641, basal view showing basal cavity (IY97-21); **B**, CNP1115, lateral view (IY97-27). **C-F**, Sb element; **C-D**, CNP1116, CN641, **C**, inner lateral view (IY96-20); **D**, basal view (IY96-19); **E-F**, CNP1117, CN641, **E**, upper view, showing cross section of cusp (IY108-30), **F**, outer lateral view (IY108-028). **G-J**, Sc element; **G-I**, CNP1118, CN641, **G**, outer lateral view (IY108-22), **H**, basal view (IY108-23), **I**, upper view, close up showing cross section of the cusp (IY108-24); **J**, CNP1119, CN641, inner lateral view (IY96-17). **K-M**, Sd element, CNP1120, CN917, **K**, outer lateral view (IY109-35), **L**, inner lateral view (IY109-37), **M**, upper view, close up showing cross section of the cusp (IY109-36). **N-R**, Pb element; N-P, CNP1121, CN641, **N**, inner lateral view (IY108-06), **O**, upper view, close up showing cross section of the cusp (IY108-07), **P**, basal view (IY108-05); Q, CNP1122, CN641, upper view, close up showing cross section of the cusp (IY108-15); *(continued opposite)*

reclined cusp and posteriorly more extended base. Sc element (Fig. 5G-J) strongly asymmetrical and laterally compressed, cusp suberect with a sharp anterior margin, a costate posterior margin and typically multicostate lateral faces; lateral costae posteriorly located, typically two to four costae on the outer lateral face and one to three costae on the inner lateral face; base more or less rectangular in lateral view (Fig. 5G) with strongly curved basal margin. Sd element resembles Sa, but is weakly asymmetrical, typically with two costae on each side (Fig. 5K-M). Pb element asymmetrical having a recurved cusp and a short base; cusp arrow-like in cross section (Fig. 5O, Q) with a sharp anterior margin, a sharply costate posterior margin, and a posterolateral costa on each side; in some specimens the costa on the inner lateral side becoming weaker (Fig. 5O); basal cavity flared in the posterior part and anteriorly narrower and inverted (Fig. 5P) with strongly curved basal margin (Fig. 5N, R).

Remarks. Bicostate symmetrical Sa (Fig. 5A-B), bicostate asymmetrical Sb (Fig. 5C-F), multicostate Sc (Fig. 5G-J), weakly asymmetrical Sd (Fig. 5K-M) and short based Pb (Fig. 5N-R) elements are recognised in the Thompson Creek material. Although no M and Pa elements have been recovered, this species can be closely compared with well documented *D. reclinatus* from Sweden (Löfgren & Tolmacheva 2003), except that the New Zealand species bears more than one costa on the lateral face of the Sc and Sd elements.

These specimens differ from associated *Protopanderodus* sp. cf. *P. varicostatus* in being generally larger in size with a more extended base, and in having costae located only on the posterior half of each side. Although they show some resemblance to those referred to *Protopanderodus* sp. from the Weemalla Formation in central New South Wales (Zhen & Percival 2004b), all the elements (including Sa, Sb and Sc) from the Weemalla Formation are multicostate.

Drepanoistodus Lindström, 1971

Type species. *Oistodus forceps* Lindström, 1955.

Drepanoistodus costatus (Abaimova, 1971) (Fig. 6A-P)

1971 *Drepanodus costatus*; Abaimova, p. 490, pl. 10, fig. 6, text-fig. 3
1976 *Scolopodus cornutiformis*; Lee, p. 172, pl. 2, fig. 18.
1981 *Drepanodus pitjanti*; Cooper, p. 162, pl. 26, figs 3-5, 7, 8.
1981 *Scolopodus flexilis*; An, p. 216, pl. 3, figs 1, 2.
1984 *Scolopodus ordosensis*; Wang & Luo, p. 284, pl. 4, figs 22, 23.
1993 *Drepanoistodus costatus* (Abaimova); Stait & Druce, p. 303, figs 12L-M, 17J, K, M, N, ?L (cum syn.).
2003 *Drepanoistodus costatus* (Abaimova); Zhen *et al*., p. 191, fig. 15A-R (cum syn.).

Material. 42 specimens from sample CN641 (see Table 1).

Description. M element makellate (Fig. 6A-D), geniculate with an antero-posteriorly strongly compressed cusp and a short base with arched basal margin in posterior or anterior view (Fig. 6A, C); cusp robust, distally curved posteriorly with a smooth anterior face (Fig. 6A), a strong costa on the posterior face (Fig. 6C) and sharp inner and outer lateral margins; outer lateral proto-process short with a length less than the maximum width of the cusp, and with a straight (Fig. 6C) or slightly arched (Fig. 6A) upper margin.

Sa element (Fig. 6E-G) symmetrical with an erect cusp bearing sharp anterior and posterior margins, a flared base and costate lateral faces, typically with one sharp costa (Fig. 6E), but some have two or more costae.

Sb element (Fig. 6H-J) weakly asymmetrical with a suberect or reclined cusp and sharp anterior and posterior margins; cusp laterally costate with a more convex outer lateral face and a concave inner lateral face.

Sc element (Fig. 6K-M) asymmetrical, strongly laterally compressed, basal cavity only flared in the posterior portion and narrowing anteriorly (Fig. 6L).

Sd element (Fig. 6N-P) asymmetrical with a reclined cusp and flared base; cusp with a convex outer lateral face bearing a sharp costa, a slightly

R, CNP1123, CN641, outer lateral view (IY108-12). **S-AA**, *Drepanoistodus tablepointensis* Stouge 1984. All from CN641. **S-T**, Sa element, **S**, CNP1124, lateral view (IY99-07); **T**, CNP1125, upper view (IY99-08). **U**, Sb element, CNP1126, outer lateral view (IY99-19). **V-W**, Sc element, CNP1127, **V**, basal view (IY109-07), **W**, outer lateral view (IY109-10). **X**, Sd element, CNP1128, inner lateral view (IY99-15). **Y-Z**, P element; **Y**, CNP1129, outer lateral view (IY99-11); **Z**, CNP1130, basal view (IY99-09). **AA**, M element, CNP1131, posterior view (IY109-06). Scale bars 100 µm.

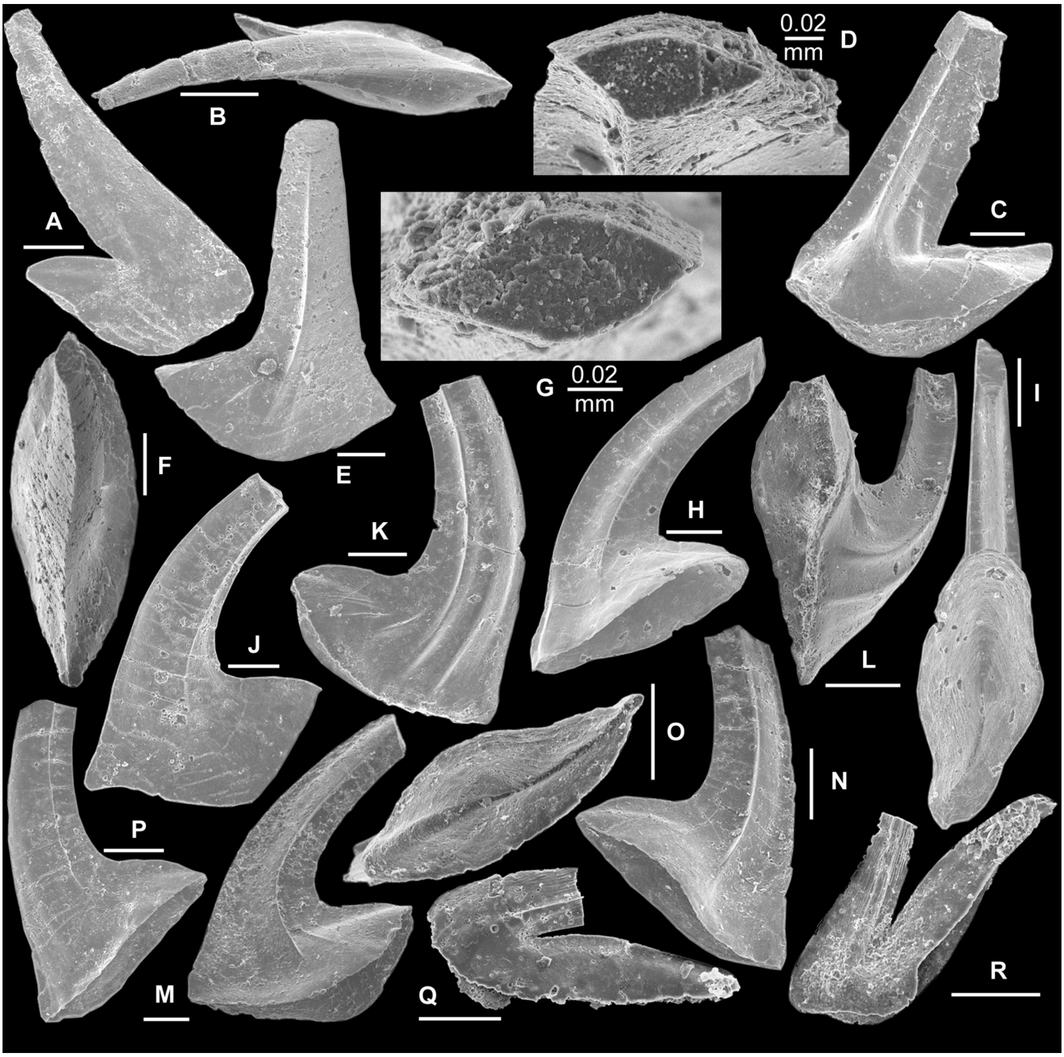

Fig. 6. **A-P**, *Drepanoistodus costatus* (Abaimova, 1971). **A-D**, M element, **A**, CNP1132, anterior view (IY93-33); **B**, CNP1133, upper view (IY98-39); **C-D**, CNP1134, **C**, posterior view (IY93-30); **D**, upper view showing cross section of the cusp (IY93-31). **E-G**, Sa element, CNP1135, **E**, lateral view (IY98-33); **F**, basal view (IY98-32); **G**, upper view showing cross section of the cusp (IY98-34). **H-J**, Sb element, **H-I**, CNP1136, **H**, inner lateral view (IY99-04); **I**, basal view (IY99-03); **J**, CNP1137, outer lateral view (IY99-05). **K-M**, Sc element, **K-L**, CNP1138, **K**, outer lateral view (IY99-01); **L**, basal view (IY99-02); **M**, CNP1139, inner lateral view (IY98-40). **N-P**, Sd element, CNP1140, **N**, inner lateral view (IY99-23); **O**, basal view (IY99-22); **P**, outer lateral view (IY99-24). **Q-R**, *Venoistodus balticus* Löfgren, 2006. All from CN641. **Q**, CNP1141, anterior view (IY109-04); **R**, CNP1142, posterior view (IY109-05). Scale bars 100 µm, unless otherwise indicated.

concave inner lateral face, and sharp anterior and posterior margins; basal cavity more strongly flared inwards.

Remarks. The material from Thompson Creek resembles that from the Lower Ordovician of Mount Arrowsmith in western New South Wales (Zhen *et al*. 2003), and is considered conspecific although minor differences do occur. For instance, the M element from Thompson Creek has a slightly longer outer lateral proto-process and a more strongly arched basal margin; the Sa element has a slightly less flared base and typically has one sharp costa on each side. However, some specimens of the Sa element display multiple costae which are identical with those from the older Tabita Formation (*evae* Zone) of western New South Wales (Zhen *et al*. 2003, fig. 15A-D). The Sc and Sd elements from Thompson Creek typically have only one costa on each lateral face (except for the Sc element which occasionally has a bicostate outer lateral face) whereas, in the Tabita material, both Sb and Sc elements often have a bicostate outer lateral face, but the second costa is normally much shorter. The Sb element from the Tabita Formation has a cusp with a gently curved posterior margin and which is distally reclined.

Specimens referred to *Drepanoistodus*? cf. *venustus* from the lower to middle part of the Table Head Formation (Middle Ordovician) of western Newfoundland (Stouge 1984) also bear strong costae on the S and M elements. Stouge (1984) suggested that *D. costatus* differed from his *D.*? cf. *venustus* in being hyaline and by having a shorter base in the M element. Rasmussen (2001) included the Table Head Formation material described by Stouge (1984) in *Drepanoistodus venustus* (Stauffer, 1935) with reservation considering that, on his interpretation, "*D. venustus*" might be separated into two species based on the occurrence of costae on the drepanodiform elements. More recently, Löfgren (2006) proposed a new genus and species *Venoistodus balticus* to accommodate specimens, mainly from Baltoscandia, which were previously assigned to *Oistodus venustus* or *O.* cf. *venustus*. *Venoistodus* was differentiated from *Drepanoistodus* mainly in lacking P elements and by its small albid elements (see further discussion under *V. balticus*). Löfgren (2006) suggested that *V. balticus* might have evolved from the Early Ordovician *Drepanoistodus forceps*. She also doubtfully considered Stouge's (1984) *D.*? cf. *venustus* from the Table Head Formation, which also lacks P elements, to be conspecific with *V. balticus*. Interestingly, no P elements have been recognised for *D. costatus* in material from either western New South Wales (Zhen *et al*. 2003) or Thompson Creek (this study). Although *D. costatus* might therefore be assigned to *Venoistodus*, its dominantly hyaline large-sized elements support its retention as a species of *Drepanoistodus*.

Drepanoistodus tablepointensis Stouge, 1984 (Fig. 5S-AA)

1984 *Drepanoistodus tablepointensis*; Stouge, p. 54-55, pl. 4, figs 9-17.

Material. 47 specimens from two samples (see Table 1).

Remarks. Specimens from Thompson Creek are comparable with the type material of this species from the Table Head Formation (Middle Ordovician) of western Newfoundland (Stouge 1984). The P element (Fig. 5Y-Z) is identical with one of the paratypes (Stouge 1984, pl. 4, fig. 14) with weaker development of the anticusp-like antero-basal corner, which was better developed in one of other illustrated paratypes (Stouge 1984, pl. 4, fig. 13). The M element is also identical with one of the illustrated paratypes (Stouge 1984, pl. 4, fig. 15) with a rounded basal-inner lateral corner, although this feature in the holotype (Stouge 1984, pl. 4, fig. 10) and the other illustrated paratypes (Stouge 1984, pl. 4, figs 16-17) is much less rounded.

Gen. et sp. indet (Fig. 3D-K)

Material. Twelve specimens (S elements) from four samples (see Table 1).

Description. Specimens referable to Sa, Sb, Sc and ?Sd elements all have a long and high posterior process with closely spaced (or even confluent), strongly laterally compressed denticles, which often bear a prominent costa on each side. Sa element alate with a cusp only slightly larger than the adjacent denticles on the posterior process; cusp T-shaped in cross section formed by intersecting blade-like costae, one on the posterior margin and the other on the anterolateral corner of each lateral side, costae on the anterolateral corner extend downwards into the short adenticulate processes (Fig. 3D). Sb element like Sa, but asymmetrical; cusp more or less Y-shaped in cross section, with a broad and concave anterior face, and a blade-like costa on each anterolateral corner extending downward to form a short blade-like adenticulate process (Fig. 3E-G). Sc element dolabrate, asymmetrical and strongly laterally compressed, with a long denticulate posterior process, a long downwardly extending anticusp, and an inwardly curved anterior margin (Fig. 3H). Sd element dolabrate, nearly symmetrical with a prominent cusp, a long denticulate posterior process and a long, downwardly extending anticusp; cusp laterally compressed with sharp anterior and posterior margins and a prominent costa on each lateral face; denticles on the posterior process strongly laterally compressed, closely spaced, posteriorly reclined and similar in size (Fig. 3I-K).

Remarks. Due to the limited material available which lacks both P and M elements, neither the genus nor species is determinable. All four elements recovered are strongly laterally compressed with costate denticles on the posterior process. The most distinctive character of this species is the development of a strong blade-like anterolateral costa (process) on each side of the

Sa and Sb elements. This feature is comparable with those in the S elements of *Cooperignathus* and *Fahraeusodus* of the Early Ordovician (see Stouge & Bagnoli 1988; Zhen *et al*. 2003). The Sd element somewhat resembles the S elements of *Paracordylodus gracilis* from the Early Ordovician (Zhen *et al*. 2004a), but the latter has pointed denticles of variable size that are less closely spaced on the posterior process, and a wider and more strongly compressed anticusp in lateral view.

Histiodella Harris, 1962

Type species. *Bryantodina sinuosa* Graves & Ellison, 1941.

Histiodella holodentata Ethington & Clark, 1982 (Fig. 2O)

1982 *Histiodella holodentata*; Ethington & Clark, p. 47-48, pl.4, figs 1, 3, 4, 16 (cum syn.).
1984 *Histiodella holodentata* Ethington & Clark; Nowlan & Thurlow, pl. 1, figs 1, 3, 5.
1998 *Histiodella tableheadensis* Stouge; Zhang, p. 72, pl. 9, figs 14, 15 (cum syn.).
2000 *Histiodella holodentata* Ethington & Clark; Zhao *et al*., p. 205, pl. 27, figs 12-1.
2001 *Histiodella kristinae* Stouge; Rasmussen, p. 82, pl. 7, figs 18, 19.
2004a *Histiodella kristinae* Stouge; Zhen *et al*., p. 97-98, fig. 14A-L.
2005 *Histiodella holodentata* Ethington & Clark; Du *et al*., p. 365, pl. 1, figs 22-26, 28 (cum syn.).
2007 *Histiodella holodentata* Ethington & Clark; Percival & Zhen, p. 391, pl. 1, figs 22-23.

Material. One specimen from sample 1-39.

Remarks. Based on material from the Table Head Formation (Middle Ordovician) of western Newfoundland, Stouge (1984, p. 18, fig. 17) established three species of *Histiodella* which were believed to form an evolutionary lineage, from oldest *H. tableheadensis* with a prominent cusp, through *H. kristinae* and then to *H. bellburnensis* with an inconspicuous cusp. As suggested by Rasmussen (2001) and Du *et al*. (2005), *H. tableheadensis* is a junior subjective synonym of *H. holodentata* Ethington & Clark, 1982. This is further supported by the original synonymy lists of both species given by the original authors (see Stouge 1984, p. 87-88; Ethington & Clark 1982, p. 47), which shared most of the junior synonyms. Although Stouge's work was published two years after that of Ethington & Clark (1982), it seems clear that the latter was not available to Stouge when he completed his study on the Table Head faunas. The holotypes of these two species are nearly identical, with a prominent cusp and a short posterior process with six denticles almost overlapping each other and forming a steeply sloping upper margin to the posterior process. They are both rectangular in outline and have a similar height:length (H:L) ratio (0.64 for the holotype of *H. holodentata*, and 0.7 for the holotype of *H. tableheadensis*). Two illustrated paratypes of *H. holodentata* (Ethington & Clark, 1982, pl. 4, figs 1, 4) bear up to ten denticles on the posterior process and have a similar H:L ratio (varying from 0.67 to 0.7). However, the illustrated paratypes of *H. tableheadensis* exhibit a wider variation; two of them (Stouge 1984, pl. 18, figs 8, 13) are identical with the holotype, but another illustrated paratype (Stouge 1984, pl. 18, fig. 12) shows a more elongate outline in lateral view with shorter denticles and a shorter cusp, with H:L ratio of 0.51, within the range for *H. kristinae* (0.50-0.58). This latter specimen occupies an intermediate position between *H. tableheadensis* (=*H. holodentata*) and *H. kristinae*, shown by its more elongate outline compared to the holotype of *H. kristinae*, but with its higher robust cusp closely resembling that of the holotype of *H. tableheadensis*.

This raises the question as to what criteria serve to distinguish *H. holodentata* from *H. kristinae* which a brief review of the literature suggests are vague and arbitrary. Zhen & Percival (2004a) used the H:L ratio to differentiate these two species, with *H. kristinae* having a more elongate outline (H:L ratio = 0.50-0.58), and on this basis referred specimens from the Oakdale Formation in central New South Wales to *H. kristinae*, although most of those have the tip of the cusp slightly higher than the highest denticles on the anterior process. However, examination (by the senior author in 2008) of abundant material of several species of *Histiodella* documented by Du *et al*. (2005) from the Tarim Basin, and correspondence with other conodont specialists (O. Lehnert 2007; S. Bergström 2009) support the concept (as originally proposed by Stouge 1984) that the relative size and height of the cusp might be a more reliable means of distinguishing *H. holodentata* from *H. kristinae*. If the original definition of *H. kristinae* given by Stouge (1984) is adhered to, whereby the cusp has its tip lower than the tips of the highest denticles on the anterior process, then the material from Thompson Creek (as well as that from the Oakdale Formation of central New South Wales, previously identified as *H. kristinae*), should be assigned to *H. holodentata* (see Percival & Zhen 2007, pl. 1, figs 22-23). Furthermore, specimens previously referred to as *H. holodentata* but with the cusp tip lower than the highest denticles on the anterior process (e.g. Rasmussen 2001, pl. 7, fig. 19) would have to be re-assigned to *H. kristinae*.

Microzarkodina Lindström, 1971

Type species. Prioniodina flabellum Lindström, 1955.

Microzarkodina sp. (Fig. 3L-M)

Material. One P element from sample 1-39, and one Sb element from sample CN641.

Remarks. Only two specimens, the angulate P element and tertiopedate Sb element, were recovered. The P element (Fig. 3L) is pastinate with a prominent cusp, a short anterior process with a single denticle, and a longer posterior process bearing five closely spaced, strongly reclined denticles. This element resembles the P element of *M. flabellum* (Lindström, 1955) (compare with Löfgren 1978, pl. 11, figs 27, 28, 32) and *M. hagetiana* Stouge & Bagnoli, 1990 (see Löfgren 2003, fig. 9AD), but differs in having a reclined cusp and strongly reclined denticles on the posterior process. The Sb element (Fig. 3M) is tertiopedate, weakly asymmetrical with a long posterior process and a lateral process on each side. Due to the limited material, it is uncertain if both elements represent a single species.

Oistodus Pander, 1856

Type species. Oistodus lanceolatus Pander, 1856.

Oistodus sp. cf. O. lanceolatus Pander, 1856 (Fig. 7A-X)

cf. 1955 *Oistodus lanceolatus* Pander; Lindström, p. 577, pl. 3, figs 58-60.
cf. 1955 *Oistodus delta*; Lindström, p. 573, pl. 3, figs 3-9.
cf. 1955 *Oistodus triangularis*; Lindström, p. 581, pl. 4, figs 14-18.
cf. 1974 *Oistodus lanceolatus* Pander; Lindström, in Ziegler, p. 201, *Oistodus*–plate 1, figs 1-3.
cf. 1988 *Oistodus lanceolatus* Pander; Bergström, pl. 2, figs 17-19.
cf. 1988 *Oistodus* aff. *O. lanceolatus* Pander; Bagnoli *et al*., p. 211, pl. 40, figs 1-4.
cf. 1988 *Oistodus* aff. *O. lanceolatus* Pander; Stouge & Bagnoli, p. 123, pl. 6, figs 1-8.
cf. 1993 *Oistodus lanceolatus* Pander; Löfgren, fig. 6V-X.
cf. 1994 *Oistodus lanceolatus* Pander; Löfgren, fig. 6.38-6.40.
cf. 2001 *Oistodus lanceolatus* Pander; Tolmacheva & Fedorov, fig. 4O-R.

Material. 172 specimens from four samples (see Table 1).

Description. M element makellate (Fig. 7A-C), geniculate with a robust cusp and a prominent adenticulate outer-lateral proto-process bearing a gently arched upper margin; cusp strongly antero-posteriorly compressed with a broad, smooth anterior face, typically a weak carina developed on the posterior face (Fig. 7C), and with sharp inner and outer lateral edges; basal margin curved with basal cavity flared posteriorly to form a weak buttress.

Sa element (Fig. 7D-G), symmetrical, tricostate, with a flat anterior face (Fig. 7G), a blade-like costa on each anterolateral side and a blade-like posterior costa (Fig. 7D); cusp T-shaped in cross section, and posteriorly curved distally (Fig. 7F); anterior face wide, almost an equilateral triangle in anterior view (Fig. 7G), with a short, weakly developed anterior costa near the base becoming a weakly developed carina upwards on the cusp (Fig. 7E); base T-shaped with shallow, nonflared basal cavity, and gently arched basal margin in anterior view; basal ledge well developed above the basal margin on posterior face (Fig. 7D).

Sb element (Fig. 7H-J) asymmetrical, with a robust cusp and an antero-posteriorly extended base; cusp suberect to reclined, triangular in cross section with a sharp costa along its anterior and posterior margins, and a sharp costa on the outer lateral face (Fig. 7I); three costae extending downwards and merging with the upper margin of the three adenticulate, blade-like proto-processes; inner lateral face concave, often with a broad carina (Fig. 7J) or a weak costa; anterior margin slightly curved inwards, forming an angle of less than 90° with the outer lateral proto-process; basal cavity shallow, extending as three narrow grooves underneath each proto-process (Fig. 7H).

Sc element (Fig. 7K-L) asymmetrical and laterally compressed, with a robust cusp and a posteriorly extended base; cusp reclined with sharp anterior and posterior margins, with smooth, convex outer lateral face (Fig. 7L) and concave inner lateral face typically with a prominent carina or weak costa (Fig. 7K); posterior proto-process with an arched upper margin; basal cavity shallow, extending anteriorly and posteriorly as a narrow groove.

Sd element (Fig. 7M-R) asymmetrical, like Sb element, but with a posteriorly more strongly curved cusp bearing two costa on each side (Fig. 7O, R); cusp typically recurved, bearing

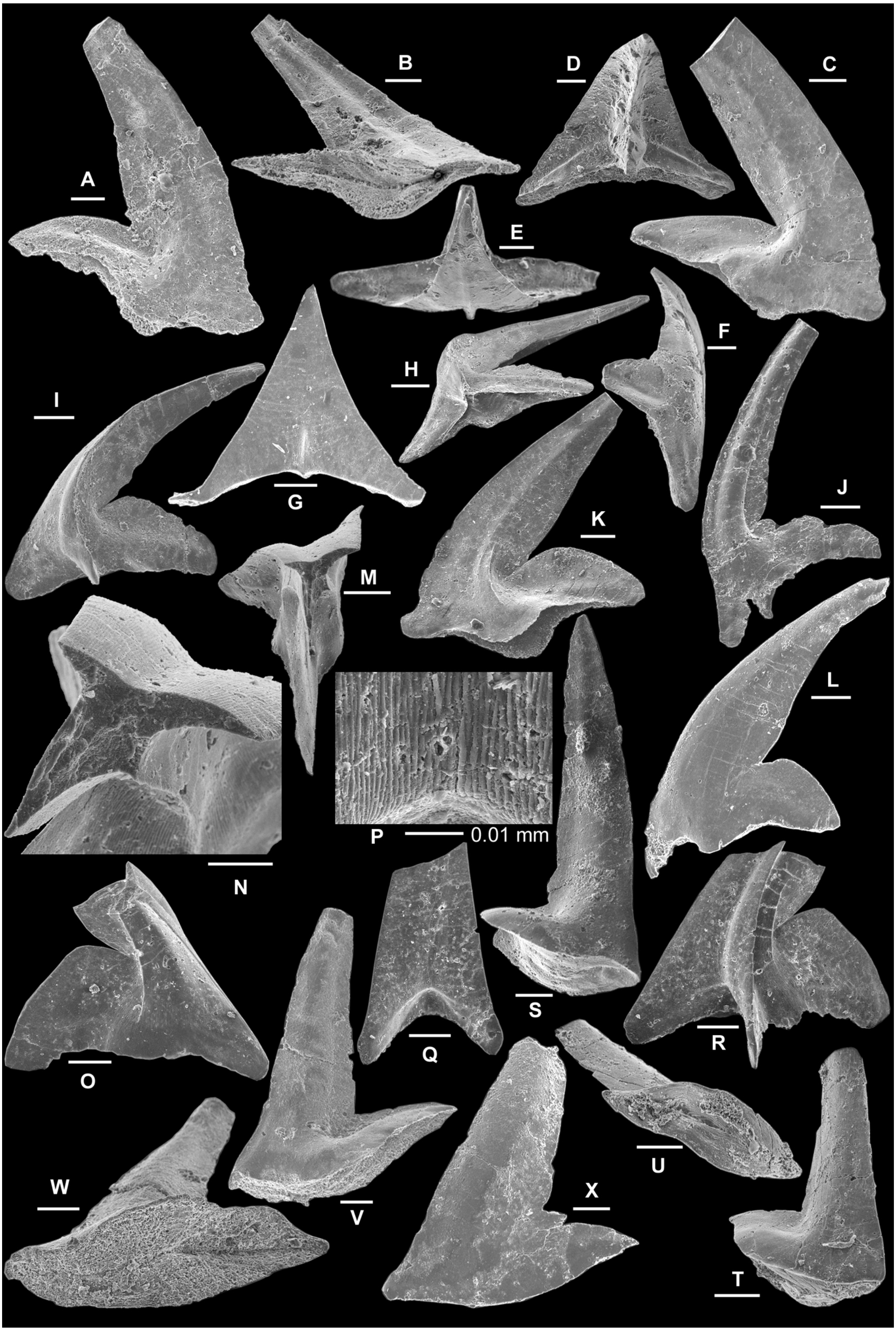
A
B
D
C
E
F
H
I
G
K
J
M
L
P
0.01 mm
N
Q
S
R
O
U
W
V
X
T

a strong blade-like costa on each anterolateral corner, which extends basally into an adenticulate proto-process, and a prominent second costa on each side; second costa on the inner lateral face typically more prominent (Fig. 7N); anterior face broad (Fig. 7Q) and V-shaped formed by the blade-like anterolateral process on each side (Fig. 7N, R).

Pa element (Fig. 7S-U) scandodiform, with an erect cusp and a short base; cusp robust, laterally compressed with sharp anterior and posterior margins and smooth lateral faces; basal cavity shallow, flared inwards (Fig. 7U).

Pb element (Fig. 7V-X), like Pa but with more laterally compressed cusp, a short anticusp-like antero-basal corner, which is triangular in lateral view, and a larger base which extends more towards the anterior and posterior (Fig. 7W).

Remarks. Before the multi-element concept of *Oistodus* was proposed by Lindström (1971, in Ziegler 1974), *Oistodus* was widely used as a form species to include oistodiform elements, which are M elements of apparatuses belonging to different conodont genera. Lindström (1971, in Ziegler 1974) defined *Oistodus* as having hyaline multielements, with *O. lanceolatus*, the type species, consisting of a trimembrate apparatus, including a two-edged element (cordylodiform= M element herein), three-edged asymmetrical element (cladognathodiform= Sb), and three-edged symmetrical element (trichonodelliform= Sa). Tolmacheva (2006) studied Pander's (1856) type material of *Scolopodus*, together with new material from one of Pander's original localities on the Popowka River, near St. Petersburg. Specimens representing M, Sa and Sb elements of *O. lanceolatus* from this locality were illustrated by Bergström (1988, pl. 2, figs 17-19). All three specimens representing the M, Sa and Sb elements illustrated by Lindström (in Ziegler 1974, p. 198-199, *Oistodus*-pl. 1, figs 1-3) were from Horns Udde (upper Latorpian), Öland, Sweden. The generic concept given by Lindström (1971, in Ziegler 1974) was followed by most subsequent workers (e.g. Serpagli 1974; Löfgren 1978; Stouge 1984; Bagnoli *et al*. 1988; Stouge & Bagnoli 1988). Bagnoli *et al*. (1988) and Stouge & Bagnoli (1988) assigned the M, P and a series of S elements to *Oistodus*. Sweet (1988, fig. 5.13) suggested a seximembrate apparatus for *Oistodus* including acodiform P element, geniculate M element, and strongly costate S elements, which form a symmetry transition series. This latter interpretation forms the basis of the current understanding of *Oistodus* with a septimembrate species apparatus including large hyaline M, Sa, Sb, Sc, Sd, Pa and Pb elements.

Van Wamel (1974), however, expanded Lindström's (1971, in Ziegler 1974) definition of *Oistodus* by including both hyaline and albid elements, arguing that hyaline elements were in association with identical elements partially or almost entirely composed of "white matter". Van Wamel also included in *Oistodus* a second species, *O. papiliosus* van Wamel, 1974, consisting of small, albid elements.

A literature review clearly shows that the definition of the species apparatus, in particular the P element, of *O. lanceolatus* (type species of the genus) varies among Ordovician workers. The specimen illustrated as the P element of *O*. aff. *O. lanceolatus* from the Cow Head Group of western Newfoundland (Stouge & Bagnoli 1988, pl. 6, figs 1, 3) closely resembles specimens assigned to the Sc element (Stouge & Bagnoli 1988, pl. 6, fig. 5), except for a more strongly extended antero-basal corner in the P element. Both the P and Sc elements defined by Stouge & Bagnoli (1988) are comparable with the Sc element applied herein. Löfgren (1993, fig. 6V-X; 1994, fig. 6.38-6.40) and Viira *et al*. (2001, fig. 5W-Y) illustrated M, Sa, Sc and P elements of *O. lanceolatus* from the Lower Ordovician (*evae* Zone) of Sweden. The P element figured by Löfgren is an asymmetrical tricostate element, equivalent to the 3-edged asymmetrical element of Lindström (1971, in Ziegler 1974), which is assigned herein to the Sb position. Tolmacheva & Fedorov (2001, fig. 4O-R) illustrated the M, Sa, Sc and P elements of *O. lanceolatus* from northwest Russia. The illustrated P element is a scandodiform element

***Fig.** 7*. *Oistodus* sp. cf. *O. lanceolatus* Pander, 1856. **A-C**, M element; **A-B**, CNP1143, CN640, **A**, posterior view (IY100-03); **B**, basal view (IY100-02); **C**, CNP1144, CN641, posterior view (IY93-26). **D-G**, Sa element; **D-F**, CNP1146, CN641, **D**, posterior view (IY93-02), **E**, upper view (IY93-04), **F**, lateral view (IY93-03); **G**, CNP1147, CN640, anterior view (IY99-35). **H-J**, Sb element, CN641; **H-I**, CNP1148, **H**, oblique, basal view (IY93-14), **I**, outer lateral view (IY93-15); **J**, CNP1149, inner lateral view (IY93-22). **K-L**, Sc element, CN641; **K**, CNP1150, inner lateral view (IY93-25); **L**, CNP1151, outer lateral view (IY93-27). **M-R**, Sd element, CN641, CNP1152, **M**, upper view (IY93-06), **N**, close up of upper view showing cross section of the cusp (IY93-05); **O**, inner lateral view (IY93-07); **P**, close up showing surface striae (IY93-10); **Q**, anterior view (IY93-09); **R**, outer lateral view (IY93-11). **S-U**, Pa element, CN641; **S**, CNP1153, inner lateral view (IY98-26); **T-U**, CNP1154, **T**, inner lateral view (IY98-29); **U**, basal view (IY98-28). **V-X**, Pb element, CN641; **V-W**, CNP1155, **V**, inner lateral view (IY93-34); **W**, basal view (IY93-35); **X**, CNP1156, outer lateral view (IY93-36). Scale bars 100 µm, unless otherwise indicated.

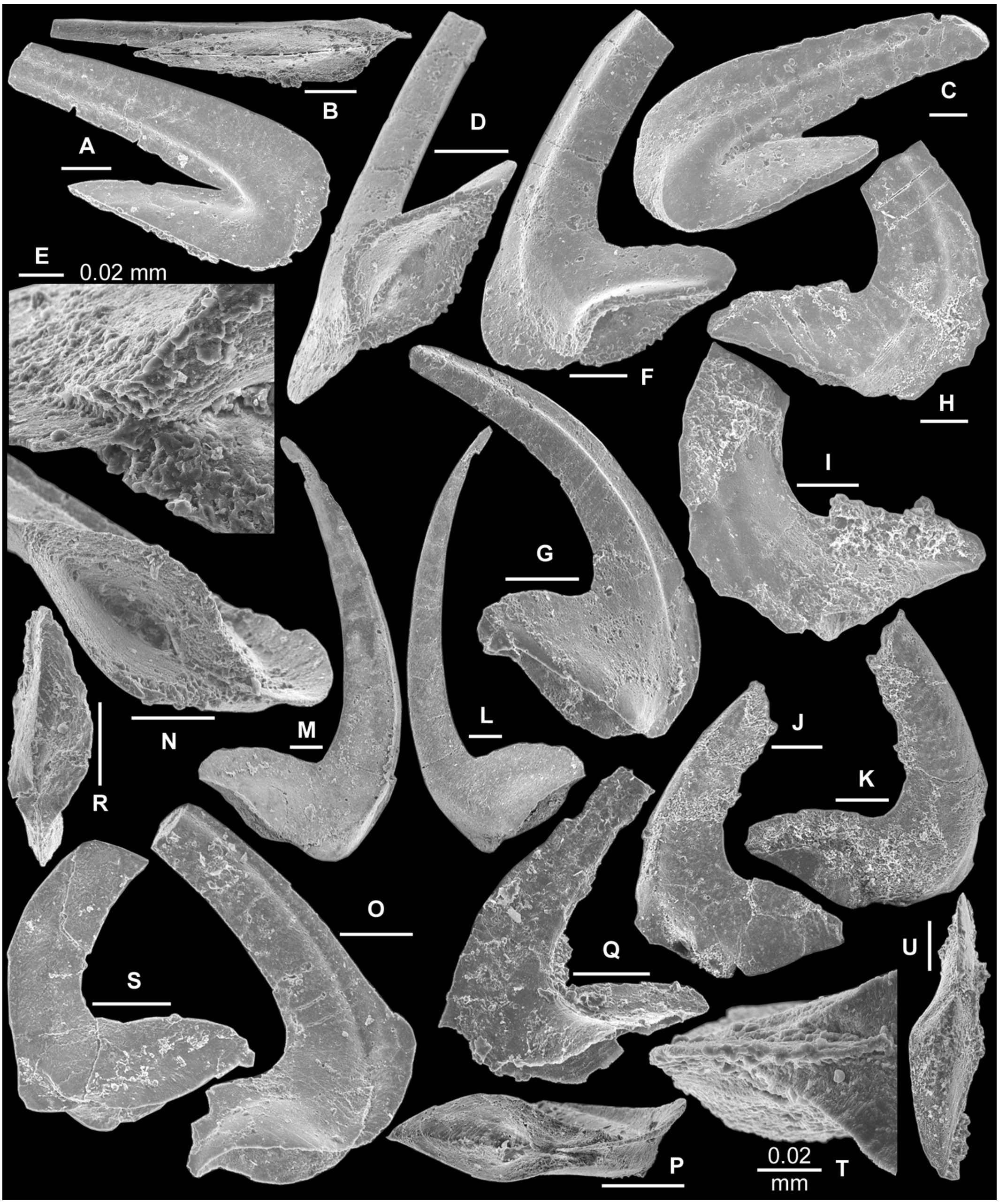

Fig. 8. *Paroistodus originalis* (Sergeeva, 1963). **A-C**, M element; **A-B**, CNP1157, CN641, **A**, posterior view (IY98-21); **B**, basal view (IY98-20); **C**, CNP1158, 1-39, posterior view (IY101-09). **D-G**, Sa element, CN641; D-F, CNP1159, **D**, basal view (IY94-38); **E**, antero-basal corner, showing anterior costa extending into base (IY94-39); **F**, lateral view (IY94-37); **G**, CNP1160, lateral view (IY98-04). **H-I**, **U**, Sb element, CNP1161, CN641; **H**, outer lateral view (IY98-03); **I**, inner lateral view (IY98-02); **U**, basal view (IY98-01). **J-K**, Sc element, CNP1162, CN641; **J**, inner lateral view (IY98-19); **K**, outer lateral view (IY98-18). **L-P**, Sd element, CN641; **L-N**, CNP1163, **L**, outer lateral view (IY98-12); **M**, inner lateral view (IY98-13); **N**, basal view (IY98-11); **O-P**, CNP1164, **O**, inner lateral view (IY98-16); **P**, basal view (IY98-17). **Q-T**, Pb element, CN641; **Q**, CNP1165, inner lateral view (IY98-30); **R-T**, CNP1166, **R**, basal view (IY98-06); **S**, outer lateral view (IY98-08); **T**, basal view, showing anterior costa extending into basal cavity. Scale bars 100 μm, unless otherwise indicated.

with extended antero-basal corner and a broad carina on the inner lateral face which is more or less in agreement with our current interpretation of the P elements, and their Sc element shows two costae on the inner lateral side, which is comparable with the Sd element defined herein. Although Sweet (1988) suggested that the P element of *Oistodus* is acodiform, his illustration did not show the costa on the outer lateral face.

Oistodus multicorrugatus Harris, 1962 was revised by Serpagli (1974) on material from the San Juan Formation, Precordillera of western Argentina, as consisting of a trimembrate apparatus, similar to that of the stratigraphically older type species. It was differentiated from the latter mainly by the development of additional costae, the occurrence of the basal ledge, and having the posterior extension highest towards its distal end. *Oistodus tablepointensis* Stouge, 1984 from the Table Head Formation (Darriwilian) of western Newfoundland is characterised by having a longer posterior proto-process, in comparison to both *O. lanceolatus* and *O. multicorrugatus*.

The P, S and M elements recovered from the Thompson Creek samples are identical with those of *O. lanceolatus* from Sweden (Lindström, 1955, in Ziegler 1974; Löfgren 1978, 1993, 1994; Bagnoli *et al*. 1988), and Russia (Tolmacheva & Fedorov 2001), except that the M element from New Zealand has its cusp less recurved outer-laterally. Furthermore the scandodiform P elements have a smooth outer lateral face and a weakly carinate inner lateral face, and can be further subdivided into Pb elements with a prominent, triangular antero-basal extension and Pa elements with a rounded non-extended antero-basal corner. Although currently no detailed revision of *O. lanceolatus* is available in the literature and the prevailing understanding of the species concept is based on scattered material, the well preserved material from Thompson Creek may represent a separate species closely related to (if not conspecific with) the stratigraphically older *O. lanceolatus*.

Paroistodus Lindström, 1971

Type species. *Oistodus parallelus* Pander, 1856.

Paroistodus horridus (Barnes & Poplawski, 1973) (Fig. 11A-B)

1973 *Cordylodus horridus*; Barnes & Poplawski, p. 771, 772, pl. 2, figs 16-18.
2004a *Paroistodus horridus* (Barnes & Poplawski); Zhen & Percival, p. 98-101, fig. 15A-L (cum syn.).
2007 *Paroistodus horridus* (Barnes & Poplawski); Percival & Zhen, pl. 1, figs 24-26.

Material. 26 poorly preserved specimens from two samples (see Table 1).

Remarks. The Sc element with an inwardly curved anterior margin, and the Pb element with a twisted posterior process, are comparable with those recently described from allochthonous limestone blocks within the Oakdale Formation of central New South Wales (Zhen & Percival 2004a).

Paroistodus originalis (Sergeeva, 1963) (Fig. 8A-U)

1963 *Oistodus originalis*; Sergeeva, p. 98, pl. 7, figs 8-9, text-fig. 4.
1971 *Oistodus originalis* Sergeeva; Lindström, p. 48, fig. 8.
1997 *Paroistodus originalis* (Sergeeva); Löfgren, p. 926-927, pl. 1, figs 13-16, 18-20, 22-33, text-fig. 5H-O (cum syn.).
2000 *Paroistodus originalis* (Sergeeva); Albanesi & Barnes, fig. 5.20-5.24.
2004b *Paroistodus originalis* (Sergeeva); Zhen & Percival, fig. 5A-B.

Material. 106 specimens from six samples (see Table 1).

Remarks. Löfgren (1997) revised the species by recognising a septimembrate apparatus including makellate M, drepanodiform S (Sa, Sb, Sc and Sd) and P (Pa and Pb) elements. S and P elements of *P. originalis* in the Thompson Creek material illustrated herein can be morphologically differentiated from typical drepanodiform elements by having a "sharp anterior costa which extends basally into the basal cavity and forms a ridge-like structure" (Zhen *et al*. 2007, p.137) at the anterior end of the basal cavity (Fig. 8E, T, here termed paroistodiform). This distinctive character is also present in the Swedish specimens of *P. proteus* (Löfgren, 1997, Zhen *et al*. 2007, pl. 5, figs 3, 7-8).

The M element generally shows a prominent carina on its anterior and posterior faces with a well rounded basal-inner lateral corner. The Sa element is symmetrical with a rather prominent carina on each lateral face and a large, thin antero-basal corner, and with basal cavity limited to the posterior part of the base. The Sb element is asymmetrical with concave inner and convex outer faces, less extended antero-basal corner, and with anterior margin flexed inwards. Löfgren (1997) observed that in the Swedish material, the Sc element is strongly compressed with an extended, more or less rhombic base in lateral

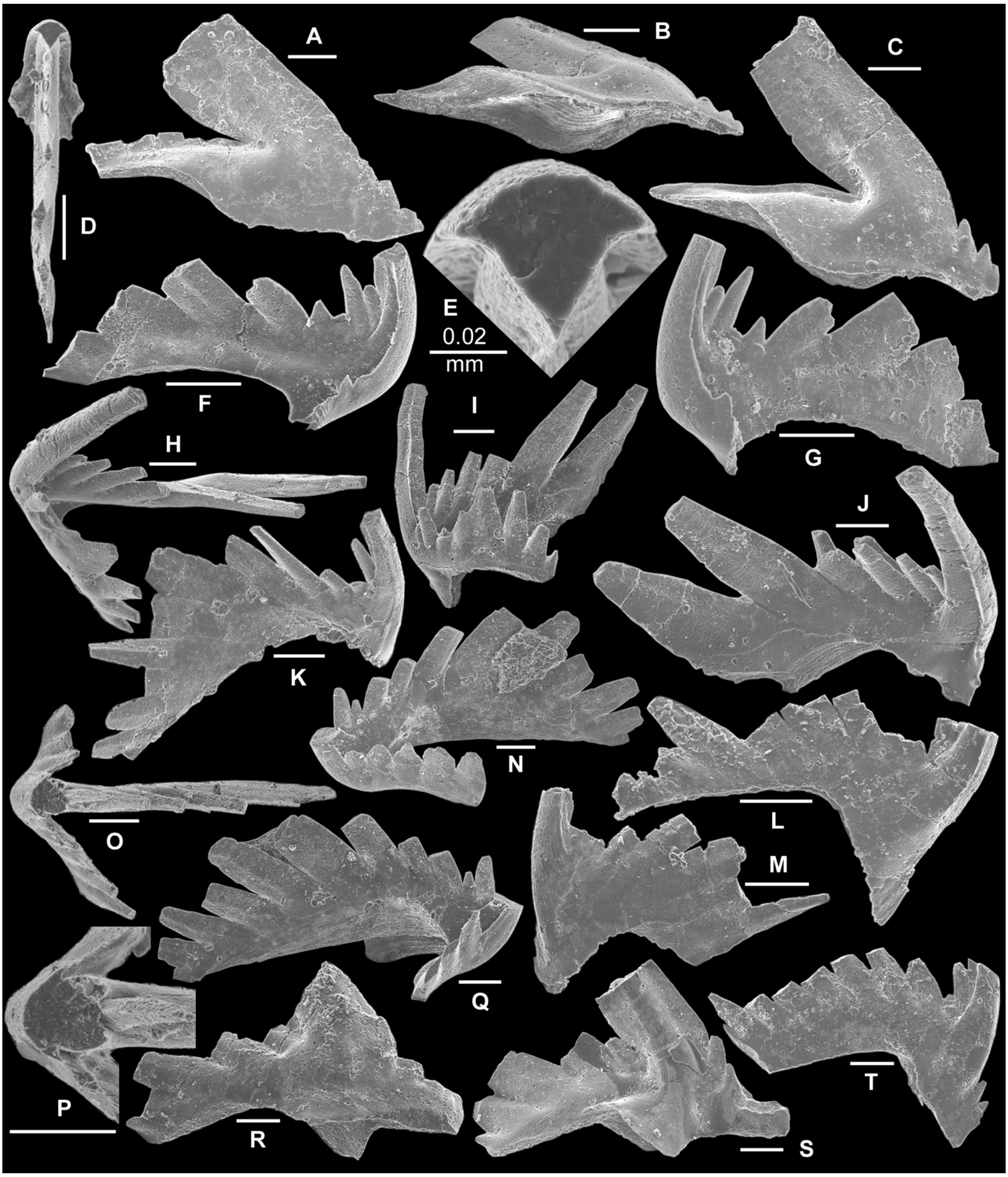

Fig. 9. *Periodon macrodentatus* (Graves & Ellison, 1941). **A-C**, M element; **A**, CNP1167, posterior view (IY95-05); **B-C**, CNP1168, **B**, basal view (IY95-03); **C**, anterior view (IY95-04). **D-G**, Sa element, CNP1169, **D**, upper view (IY95-10), **E**, upper view showing symmetrical cross section of the cusp (IY95-11); **F-G**, lateral views (IY95-12, IY95-13). **H-K**, Sb element; **H-J**, CNP1170, **H**, upper view (IY95-15); **I**, outer lateral view (IY95-16); **J**, inner lateral view (IY95-18); **K**, CNP1171, inner lateral view (IY95-30). **L-M**, Sc element; **L**, CNP1172, inner lateral view (IY95-31); **M**, CNP1173, outer lateral view (IY96-06). **N-Q**, Sd element, CNP1174, **N**, **Q**, lateral views (IY95-19, IY95-20); **O**, upper view (IY95-21); **P**, upper view, close up showing asymmetrical cross section of the cusp (IY95-22). **R-S**, Pa element; **R**, CNP1175, outer lateral view (IY95-08); **S**, CNP1176, inner lateral view (IY95-06). **T**, Pb element, CNP1177, outer lateral view (IY96-02). All from CN641; scale bars 100 µm, unless otherwise indicated.

view and with the basal cavity restricted to the posterior portion of the base. The Sd element is similar to the Sb but with its anterior margin strongly flexed inwards, and the base has a keeled and arched upper margin. Typical Pa elements were not recognised in the Thompson Creek samples. P elements described from Sweden (Löfgren 1997) have a flared basal cavity, with the Pa displaying a more convex outer lateral face, typically having the base more strongly flared outer laterally with a notch on the basal margin.

Periodon Hadding, 1913

Type species. Periodon aculeatus Hadding, 1913.

Periodon macrodentatus (Graves & Ellison, 1941) (Fig. 9A-T)

1941 *Ozarkodina macrodentata*; Graves & Ellison, p. 14, pl. 2, figs 33, 35, 36.
1976 *Periodon macrodentata* (Graves & Ellison); Cawood, fig. 3a.
2001 *Periodon macrodentata* (Graves & Ellison); Rasmussen, p. 114-116, pl. 14, figs 1-8 (cum syn.).
2004b *Periodon macrodentatus* (Graves & Ellison); Zhen & Percival, p. 168-170, fig. 10A-N (cum syn.).
2007 *Periodon macrodentatus* (Graves & Ellison); Percival & Zhen, p. 392, pl. 1, figs 32-33.

Material. 204 specimens from seven samples (see Table 1).

Description. M element (Fig. 9A-C) makellate with an adenticulate outer lateral proto-process and an anticusp-like inner lateral process typically bearing two or three small denticles; cusp antero-posteriorly compressed with broad anterior (Fig. 9C) and posterior (Fig. 9A) faces, and with sharp inner and outer lateral margins; height of the cusp longer than length of the base, but the ratio of length of the base to cusp height (Lb:Hc) cannot be precisely estimated, as all specimens recovered had the cusp tip broken; basal margin sinuous.

Sa element (Fig. 9D-G) symmetrical, alate with a suberect cusp, a long denticulate posterior process, and a denticulate lateral process on each side; cusp resembles an isosceles triangle in cross section with a broad and rounded anterior face and an angular costa at each anterolateral corner and along the posterior margin (Fig. 9E); three sharp costae extend downward to merge with the upper margin of the processes (Fig. 9D); denticles on the posterior process laterally compressed, progressively more strongly reclined and larger in size away from the cusp; lateral processes typically broken in the specimens recovered, with small, rudimentary denticles on the upper edge (Fig. 9F-G).

Sb element (Fig. 9H-K) modified tertiopedate, strongly asymmetrical with a long denticulate posterior process which is curved inward distally, an antero-outer lateral process, which is typically denticulate and strongly curved posteriorly (Fig. 9H), and a costa on the antero-inner lateral corner which may extend downwards as a short process with a few rudimentary denticles (Fig. 9J); some specimens have a less well developed antero-outer lateral process and only an antero-inner lateral costa on the inner lateral face (Fig. 9K).

Sc element (Fig. 9L-M) bipennate, asymmetrical, with a long denticulate posterior process and a short denticulate anterior process; cusp laterally compressed with a sharp costa along its anterior and posterior margins, a prominent costa on the outer lateral face and a carina on the inner lateral face; both the outer lateral costa and inner lateral carina do not extend to the base; anterior process often anticusp-like and posterolaterally curved with one to three small denticles; on the posterior process, two or three denticles immediately next to the cusp are much smaller than those on the distal part.

Sd element (Fig. 9N-Q) tertiopedate, like Sa but asymmetrical (Fig. 9P), with more prominent, long, denticulate lateral processes (Fig. 9O); cusp curved posterolaterally; posterior process long, varying from nearly straight to curved inwards.

Pa element (Fig. 9R-S) angulate, inwardly bowed with denticulate anterior and posterior processes; cusp robust, laterally compressed with sharp anterior and posterior margins and a broad carina on the inner lateral face; posterior process bearing five or more denticles, which are closely spaced and laterally compressed; anterior process shorter, with three or more denticles.

Pb element (Fig. 9T) bipennate with a long denticulate posterior process and a shorter downwardly extending and inwardly curved anterior process; like Sc element but the denticles on the posterior process more or less equal in size and less laterally compressed, and the basal cavity is deeper and not inverted.

Remarks. The septimembrate concept of this species was defined by Stouge (1984) under the name of *Periodon aculeatus zgierzensis* Dzik, 1976. Rasmussen (2001) was able to distinguish both *P. macrodentatus* and *P. zgierzensis* as well as three other species of *Periodon* (*P. selenopsis*, *P. flabellum* and *P. aculeatus*) from the Andersön-B Section of the upper Lower to Middle Ordovician

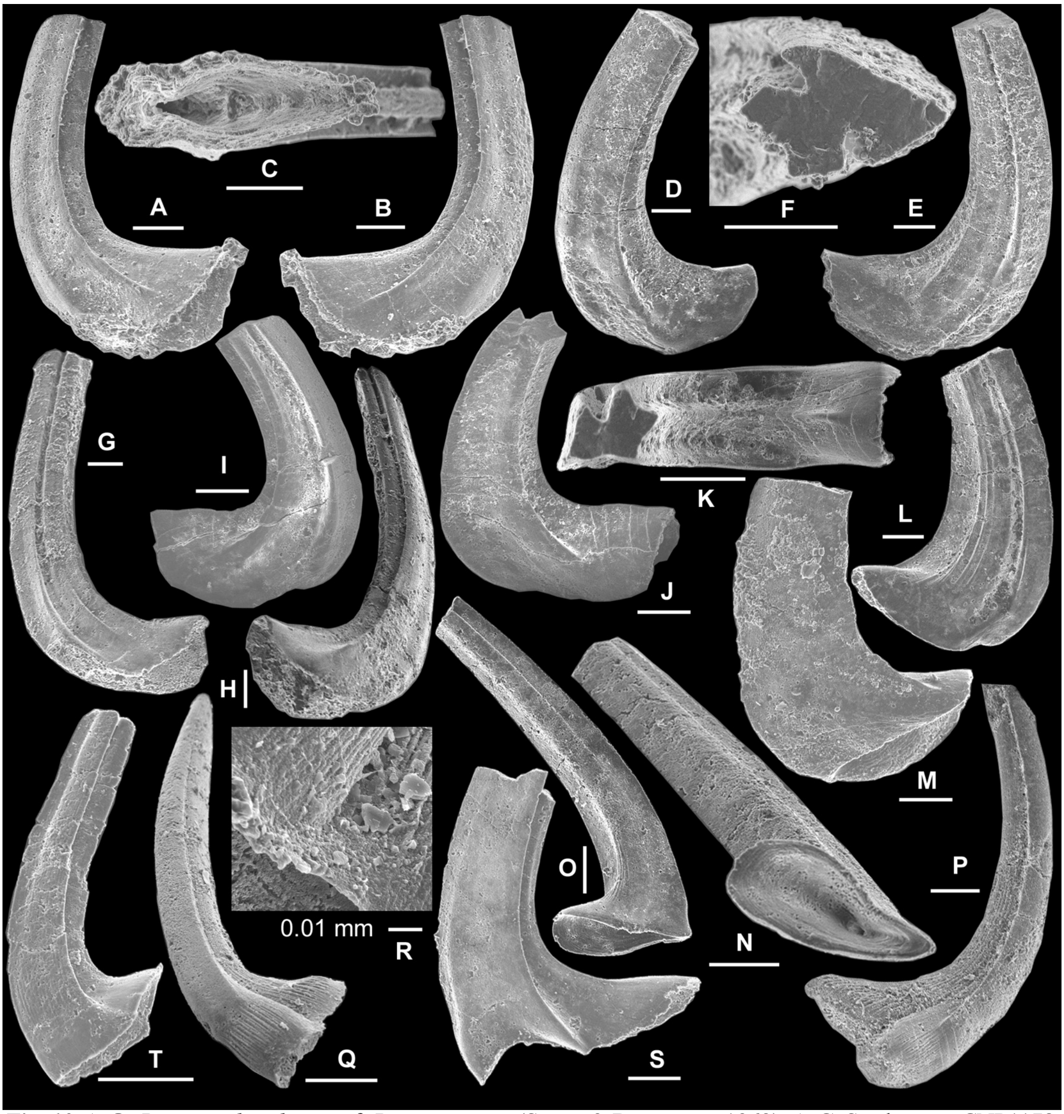

Fig. 10. **A-O**, *Protopanderodus* sp. cf. *P. varicostatus* (Sweet & Bergström, 1962). **A-C**, Sa element, CNP1178, **A, B**, lateral view (IY96-22, IY96-3); **C**, basal view (IY96-24). **D-F**, Sb element, CNP1179, **D**, outer lateral view (IY96-33), **E**, inner lateral view (IY96-32), **F**, upper view, close up showing cross section of the cusp (IY96-34). **G-H**, Sc element, CNP1180, **G**, inner lateral view (IY96-26), **H**, outer lateral view (IY96-27). **I-K**, Sd element, CNP1181, **I**, outer lateral view (IY97-14); **J**, inner lateral view (IY97-13); **K**, posterior view (IY97-11). **L-M**, Pa element; **L**, CNP1182, inner lateral view (IY96-13); **M**, CNP1183, outer lateral view (IY96-25). **N-O**, Pb element, CNP1184, **N**, posterior view (IY96-12); **O**, inner lateral view (IY96-11). **P-R**, *Protopanderodus*? *nogamii* (Lee, 1975). **P**, Sb element, CNP1185, inner lateral view (IY100-37). **Q-R**, Sa element, CNP1186, **Q**, lateral view (IY100-33); **R**, lateral view, close up showing lateral furrow not extending to the basal margin. **S**, *Protopanderodus cooperi* (Sweet & Bergström, 1962). Sa element, CNP1187, lateral view (IY99-32). **T**, *Protopanderodus rectus* (Lindström, 1955). Sa element, CNP1188, lateral view (IY101-16). All from CN641; scale bars 100 µm, unless otherwise indicated.

from the island of Andersön, Sweden.

Rasmussen's (2001) reinterpretation of the species apparatus includes the M (=oistodontiform of Stouge 1984), Sa (=triconodelliform), Sb (=loxognathiform), Sc (=cordylodontiform), Sd (=periodontiform), Pa (=prioniodiniform) and Pb (=oulodontiform). This species concept for *P. macrodentatus* was accepted by Zhen & Percival (2004b) for specimens from the Weemalla Formation of central New South Wales. The Thompson Creek material is identical with that from New South Wales, except that denticles on the inner lateral process of the M element are less well developed, typically being smaller in the New Zealand specimens. In addition, a modified tertiopedate Sb element with a denticulated antero-outer lateral process has also been recovered from Thompson Creek. By analogy with other septimembrate species apparatuses with similar construction, we are now designating the weakly asymmetrical tertiopedate element (previously Sb element of Rasmussen 2001, and Zhen & Percival 2004b) as occupying the Sd position, and assigning the strongly asymmetrical, modified tertiopedate element (Sd element of Rasmussen 2001) to the Sb position.

Protopanderodus Lindström, 1971

Type species. Acontiodus rectus Lindström, 1955.

Protopanderodus cooperi (Sweet & Bergström, 1962) (Fig. 10S)

1962 *Acontiodus cooperi*; Sweet & Bergström, p. 1221, pl. 168, figs 2, 3, text-fig. 1G.
1983 *Acontiodus cooperi* Sweet & Bergström; Burrett *et al*., p. 180, fig. 9E.
1998 *Protopanderodus cooperi* (Sweet & Bergström); Zhang, p. 81, 82, pl. 14, figs 13-17 (cum syn.).
2004b *Protopanderodus cooperi* (Sweet & Bergström); Zhen *et al*., p. 155, fig. 8A-E.
2004b *Protopanderodus cooperi* (Sweet & Bergström); Zhen & Percival, p. 170, fig. 11C-F (cum syn.).
2006 *Protopanderodus robustus* (Hadding); Mellgren & Eriksson, p. 106-108, figs 9H-N, 13A-K.

Material. Four specimens from sample CN641.

Remarks. This species is relatively rare in the current collection. It is characterised by having a well developed, high, heel-like extension at the antero-basal corner. The Thompson Creek specimens (Fig. 10S) are identical with those reported from the Gisbornian upper part of the Wahringa Limestone Member, Fairbridge Volcanics (Zhen *et al*. 2004b) and the Darriwilian Weemalla Formation (Zhen & Percival 2004b) of central New South Wales. *Protopanderodus rectus* Lindström, 1955 resembles *P. cooperi*, but differs in having a shorter base and lacking the high, heel-like anticusp (Fig. 10T).

In a recent revision of *Protopanderodus* species from the Middle Ordovician in Sweden, Mellgren & Eriksson (2006) assigned the typical *P. cooperi* to their revised *P. robustus*, which Zhen *et al*. (2009) considered to be a poorly known species, and a possible senior synonym of either *P. rectus* or *P. graeai* (Hamar, 1964).

Protopanderodus sp. cf. P. varicostatus (Sweet & Bergström, 1962) (Fig. 10A-O)

Material. 109 specimens from six samples (see Table 1).

Description. A seximembrate apparatus including scandodiform multicostate Pa and unicostate Pb, and acontiodiform S (Sa, Sb, Sc and Sd) elements with one or two costae on each side. Sa element symmetrical; cusp suberect, with a sharp costa along its anterior and posterior margins, bearing a prominent costa and a groove posterior to it on each lateral face; often a weak anterolateral carina developed on each side (Fig. 10A-C). Sb element (Fig. 10D-F) strongly asymmetrical; cusp suberect, with sharp anterior and posterior margins; outer lateral face more convex with a deep groove which is located more towards the posterior margin (Fig. 10F), bordered by a costa on each side, and becoming shallower and open towards the base; the costa bordering the anterior side is stronger (Fig. 10F); groove on the inner lateral face is about in the middle, with one costa bordering the anterior and the posterior sides of the groove, and a third weaker costa near the posterior margin (Fig. 10F). Sc element (Fig. 10G-H) like Sb element, but more strongly compressed laterally. ?Sd element (Fig. 10I-K), asymmetrical with a suberect to reclined cusp, like Sb but with a more extended base; outer lateral face bearing a deep groove with a strong costa bordering each side; inner lateral face bearing a median costa. Pa element (Fig. 10L-M) with a multicostate inner lateral face and a smooth outer lateral face; the inner lateral face typically with three or more costae bordering two grooves, base flared towards inner side. Pb element (Fig. 10N-O) bearing a single costa to form the anterior border of a groove on the inner lateral face (Fig. 10O); outer lateral face smooth, base flared posteriorly towards inner side.

Remarks. Zhen & Percival (2004a, b), Zhen *et al*. (2004b) and Zhen & Pickett (2008), assigned material of *Protopanderodus* from central New South Wales to both *P. varicostatus* and *P. calceatus* or compared it with these species. It remains unclear whether the number of lateral costae on the S element can be utilised as a reliable character to enable differentiation of these closely related species. Mellgren & Eriksson (2006) proposed a species apparatus including nine (M1, M2, Sa, Sb, Sc Sd, Pa, Pb1 and Pb2) elements for multicostate *P. calceatus*. They assigned scandodiform elements, which are widely recognised to represent the P positions, to M positions, and distinguished the S and P elements mainly on variations of costae and symmetry. The difficulties encountered in species definition of *Protopanderodus*, alluded to above, do not inspire confidence in such a reconstruction, so we retain the traditional element designations.

The Thompson Creek specimens seem to represent an intermediate form between *P. varicostatus* and *P*. cf. *calceatus* of Zhen & Percival (2004a, b). In general morphology the New Zealand species resembles material referred to *P. varicostatus* from the Weemalla Formation, except that its S elements have fewer costae on the lateral faces. Although the number of these costae is comparable to *P*. cf. *calceatus* from allochthonous blocks in the Oakdale Formation, Sa and Sb elements of the latter species have broad anterior faces instead of the sharp-edged anterior margin observed in the Thompson Creek specimens. Material referred to *P*. cf. *varicostatus* from limestone in the basal Goonumbla Volcanics of central New South Wales (Zhen & Pickett 2008) appears also to be morphologically close to *P*. cf. *calceatus*, as its Sa and Sb elements exhibit a broad anterior face, although the number of costae on the S elements are comparable with those on the Thompson Creek specimens.

Protopanderodus? nogamii (Lee, 1975) (Fig. 10P-R)

1975 *Scolopodus nogamii*; Lee, p. 179, pl. 2, fig. 13.
1988 *Protopanderodus nogamii* (Lee); Watson, p. 124, pl. 3, figs 1, 6.
2003 *Protopanderodus nogamii* (Lee); Zhen *et al*., p. 207, Fig. 23A-P, ?Q (cum syn.).
2004b *Protopanderodus? nogamii* (Lee); Zhen & Percival, p. 170, fig. 11P, Q (cum syn.).
2004 *Panderodus nogamii* (Lee); Cantrill & Burrett, p. 410-415, pl. 1, fig. 1-16.

Material. 19 specimens from four samples (see Table 1).

Remarks. This species is widely distributed in the Early (Floian) to Late (lower Katian) Ordovician in eastern Australia, China, southeastern Asia, and the Argentine Precordillera, and has been assigned to several genera by various authors. It seems to represent a taxon related to both *Protopanderodus* and *Panderodus*, but differs from the former in not having a posteriorly extended base, and from the latter in having a furrow on each side in most of the elements, though not a true panderodid furrow as in typical *Panderodus*. Specimens are relatively rare in samples from Thompson Creek, but are apparently identical with those documented from central and far western New South Wales (Zhen & Percival 2004a, b; Zhen *et al*. 2004b).

Spinodus Dzik, 1976

Type species. *Polygnathus spinatus* Hadding, 1913.

Spinodus sp. (Fig. 11C-H)

Material. 11 specimens from four samples (see Table 1).

Remarks. Only three element types assignable to *Spinodus* were recovered from the New Zealand samples, represented by a bipennate (referred to here as the Sb element) and two dolabrate (referred to here as the Sc and M) elements. The Sc element has a long posterior process bearing more than eight peg-like denticles, and an indistinct cusp, which is nearly the same size as the adjacent denticles (Fig. 11H). The M element is similar to the Sc, but with a rounded inner lateral-basal corner lacking an anticusp (Fig. 11E-G). The anterior process of the Sb element bears several peg-like denticles that are strongly curved posteriorly (Fig. 11C-D). In having more closely spaced denticles the Thompson Creek specimens can be easily distinguished from corresponding elements of the type species *S. spinatus*, and also from *S*. sp. cf. *S. spinatus* described from the Weemalla Formation of central New South Wales (Zhen & Percival 2004b).

Spinodus? sp. (Fig. 2P)

Material. One specimen CNP1094 from sample CN641.

Remarks. This dolabrate element is superficially comparable with S elements of *Cordylodus* species common in the latest Cambrian to Tremadocian. The only specimen shows wider spaced denticles on the posterior process and a more prominent anti-cusp than those referred to herein as *Spinodus* sp. (Fig. 11C-H).

Triangulodus van Wamel, 1974

Type species. Multielement *Scandodus brevibasis* (Sergeeva, 1963), subsequent designation by Lindström (1971).

Fig. 11. **A-B**, *Paroistodus horridus* (Barnes & Poplawski, 1973). **A**, Sc element, CNP1189, CN918, inner lateral view (IY101-01). **B**, Pb element, CNP1190, CN918, inner lateral view (IY101-02). **C-H**, *Spinodus* sp. All from CN641. **C-D**, Sb element; **C**, CNP1191, inner lateral view (IY95-39); **D**, CNP1192, basal view (IY95-41). **E-G**, M element; **E**, CNP1193, anterior view (IY95-40); **F-G**, CNP1194, **F**, anterior view (IY95-48); **G**, antero-basal view (IY95-47). **H**, Sc element, CNP1195, inner lateral view (IY95-33). **I-T**, *Triangulodus* sp. **I-K**, Sa element; **I**, CNP1196, CN641, upper view (IY94-10); **J-K**, CNP1197, CN641, **J**, postero-basal view (IY94-05); **K**, posterior view (IY94-04). **L-O**, Sb element; **L-M**, CNP1198, CN641, **L**, inner lateral view (IY94-14); **M**, basal view (IY94-13); **N-O**, CNP1199, CN641, **N**, upper view (IYIY94-18); **O**, upper view, showing cross section of cusp (IY94-19). **P-R**, Sc element; **P**, CNP1200, CN641, outer lateral view (IY94-23); **Q-R**, CNP1201, CN641, **Q**, outer lateral view (IY109-13), **R**, basal view (IY109-12). **S-T**, P element; CNP1202, CN642, **S**, basal view (IY100-07); **T**, inner lateral view (IY100-06). Scale bars 100 μm, unless otherwise indicated.

Triangulodus sp. (Fig. 11I-T)

Material. 43 specimens from four samples (see Table 1).

Remarks. Only Sa, Sb, Sc and P elements of this species were recovered from the Thompson Creek samples, and all are large, hyaline elements. The Sa (Fig. 11I-K) and Sb (Fig. 11L-O) elements show some resemblance to corresponding elements of *Triangulodus zhiyii* Zhen (in Zhen *et al*. 2006) from the Early Ordovician Honghuayuan Formation of South China, but have more strongly developed blade-like costae which extend basally to form prominent, adenticulate proto-processes (Fig. 11K, L-M).

Venoistodus Löfgren, 2006

Type species. *Venoistodus balticus* Löfgren, 2006

Venoistodus balticus Löfgren, 2006 (Fig. 6Q-R)

2006 *Venoistodus balticus*; Löfgren, p. 13-20, figs 2A-I, 3A-G, I-M, P-R, W-AA.

Material. Two specimens (both M elements) from one sample (see Table 1).

Remarks. Based on a large collection from the Middle Ordovician of Baltoscandia, *V. balticus* was defined by Löfgren (2006) as consisting of small, albid geniculate (M) elements and drepanodiform (S) elements, but lacking P elements. The M element of this species is distinctive with the cusp and the base nearly equal in length. It was widely distributed in the Middle Ordovician in Baltica and South China, although generally buried in the literature as the form species, "*Oistodus*" *venustus* Stauffer (see synonymy provided by Löfgren 2006). However, the North American species *Oistodus venustus* Stauffer, 1935 has now been confirmed as a species of *Oistodus* (belonging to Oistodontidae), consisting of two types of hyaline geniculate elements, based on studies of the topotype and other material from the Glenwood Formation (Leslie 2000). It is thus quite distinct from *Venoistodus* (belonging to Drepanoistodontidae), characterised by albid elements (Löfgren 2006).

ACKNOWLEDGEMENTS

Study by YYZ was partially supported by the CAS/SAFEA International Partnership Program for Creative Research Teams. SEM work was carried out at the Electron Microscope Unit of the Australian Museum. Prof. S.M. Bergström and Dr J. Repetski are thanked for their careful and constructive reviews of the manuscript. Percival publishes with the permission of the Director, Geological Survey of New South Wales, NSW Department of Primary Industries. This is a contribution to IGCP Project 503: Ordovician Palaeogeography and Palaeoclimates.

REFERENCES

Abaimova, G.P., 1971. New Early Ordovician conodonts from the southeastern part of the Siberian Platform. *Paleontological Journal 1971 (4)*, 486-493.

Albanesi, G.L. & Barnes, C.R., 2000. Subspeciation within a punctuated equilibrium evolutionary event: phylogenetic history of the Lower-Middle Ordovician *Paroistodus originalis-P. horridus* complex (Conodonta). *Journal of Paleontology 74*, 492-502.

Albanesi, G.L., Hünicken, M.A. & Barnes, C.R., 1998. *Bioestratigrafia, biofacies y taxonomia de conodontes de las secuencias Ordovicicas del cerro porterillo, Precordillera central de San Juan, R. Argentina*. Córdoba, Argentina, 249 p.

An T.X., 1981. Recent progress in Cambrian and Ordovician conodont biostratigraphy of China. *Geological Society of America Special Paper 187*, 209-226.

An T.X., 1987. *Early Paleozoic conodonts from south China*. Peking University Publishing House, Beijing, 238 p.

An T.X., Du G.Q., Gao Q.Q., Chen X.B. & Li W.T., 1981. Ordovician conodont biostratigraphy of the Huanghuachang area of Yichang, Hubei. 105-113 in Micropalaeontological Society of China, (ed.), *Selected Papers of the First Symposium of the Micropalaeontological Society of China*, Science Press, Beijing

Bagnoli, G., Stouge, S. & Tongiorgi, M., 1988. Acritarchs and conodonts from the Cambro-Ordovician Furuhäll (Köpingsklint) Section (Öland, Sweden). *Rivista Itakuaba di Paleontologia e Stratigrafia 94 (2)*, 163-248.

Balfour, F.M., 1880-1881. *A treatise on comparative embryology*. Macmillan & Co., London, vol. 1, 492 p., vol. 2, 655 p.

Barnes, C.R. & Poplawski, M.L.S., 1973. Lower and Middle Ordovician conodonts from the Mystic Formation, Québec, Canada. *Journal of Paleontology 47*, 760-790.

Bergström, S.M., 1988. On Pander's Ordovician conodonts: distribution and significance of the *Prioniodus elegans* fauna in Baltoscandia. *Senckenbergiana lethaea 69*, 217-251.

Bergström, S.M., Riva, J. & Kay, M., 1974. Significance of conodonts, graptolites, and shelly faunas from the Ordovician of Western and North-central Newfoundland. *Canadian Journal of Earth Sciences 11*, 1625-1660.

Bishop, D.G., 1965. Two new Paleozoic fossil localities in North-west Nelson. New *Zealand Journal of Geology and Geophysics 8*, 1232-1233.

Bishop, D.G., 1971. *Sheets S1, S3, and pt S4 Farewell-Collingwood (1st Ed.) Geological Map of New Zealand 1:63,360*. Department of Scientific and Industrial Research, Wellington.

Branson, E.B. & Branson, C.C., 1947. Lower Silurian conodonts from Kentucky. *Journal of Paleontology 21*, 549-556.

BURRETT, C., STAIT, B. & LAURIE, J., 1983. Trilobites and microfossils from the Middle Ordovician of Surprise Bay, southern Tasmania, Australia. *Memoirs of the Association of Australasian Palaeontologists 1*, 177-193.

CANTRILL, R.C. & BURRETT, C.F., 1994. The greater Gondwana distribution of the Ordovician conodont *Panderodus nogamii* (Lee) 1975. *Courier Forschungsinstitut Senckenberg 245*, 407-419.

CAWOOD, P.A., 1976. Cambro-Ordovician strata, northern New South Wales. *Search 7*, 317-318.

CHEN X., ZHANG Y.D., BERGSTRÖM, S.M. & XU H.G., 2006. Upper Darriwilian graptolite and conodont zonation in the global stratotype section of the Darriwilian stage (Ordovician) at Huangnitang, Changshan, Zhejiang, China. *Palaeoworld 15*, 150-170.

COOPER, B.J., 1981. Early Ordovician conodonts from the Horn Valley Siltstone, central Australia. *Palaeontology 24*, 147-183.

COOPER, R.A., 1979. Ordovician geology and graptolite faunas of the Aorangi Mine area, North-west Nelson, New Zealand. *New Zealand Geological Survey Paleontological Bulletin 47*, 1-127.

COOPER, R.A., 1989. Early Paleozoic terranes of New Zealand. *Journal of the Royal Society of New Zealand 19*, 73-112.

COOPER, R.A. & BRADSHAW, M.A., 1986. Lower Paleozoic of Nelson-Westland. *Geological Society of New Zealand Miscellaneous Publication 33C*, 1-42.

COOPER, R.A. & DRUCE, E.C., 1975. Lower Ordovician sequence and conodonts, Mount Patriarch, North-west Nelson, New Zealand. *New Zealand Journal of Geology and Geophysics 18*, 551-582.

DU P.D., ZHAO Z.X., HUANG Z.B., TAN Z.J., WANG C., YANG Z.L., ZHANG G.Z. & XIAO J.N., 2005. Discussion on four conodont species of *Histiodella* from Tarim Basin and their stratigraphic implication. *Acta Micropalaeontologica Sinica 22*, 357-369.

DZIK, J., 1976. Remarks on the evolution of Ordovician conodonts. *Acta Palaeontologica Polonica 21*, 395-455.

DZIK, J., 1994. Conodonts of the Mójcza Limestone. *Palaeontologia Polonica 53*, 43-128.

ETHINGTON, R.L. & CLARK, D.L., 1982. Lower and Middle Ordovician conodonts from the Ibex area, western Millard County, Utah. *Brigham Young University Geology Studies 28(2)*, 1-160.

FÅHRÆUS, L.E., 1966. Lower Viruan (Middle Ordovician) conodonts from the Gullhögen Quarry, Southern Central Sweden. *Sveriges Geologiska Undersökning C 610*, 1-40.

FÅHRÆUS, L.E. & HUNTER, D.R., 1985. Simple-cone conodont taxa from the Cobbs Arm Limestone (Middle Ordovician), New World Island, Newfoundland. *Canadian Journal of Earth Sciences 22*, 1171-1182.

GRAVES, R.W. & ELLISON, S., 1941. Ordovician conodonts of the Marathon Basin, Texas. *University of Missouri, School of Mines and Metallurgy, Technical Series Bulletin 14*, 1-26.

HADDING, A.R., 1913. Undre dicellograptusskiffern i Skåne jämte några därmed ekvivalenta bildningar. *Lunds Universitets Årsskrift, Ny Följd, Afdelning 2, 9 (15)*, 1-90.

HAMAR, G., 1964. Conodonts from the lower Middle Ordovician of Ringerike. *Norsk Geologisk Tidsskrift 44*, 243-292.

HARRIS, R.W., 1962. New conodonts from the Joins (Ordovician) Formation of Oklahoma. *Oklahoma Geology Notes 22*, 199-211.

HUGHES, C.P. & WRIGHT, A.J., 1970. The trilobites *Incaia* Whittard 1955 and *Anebolithus* gen. nov. *Palaeontology 13*, 677-690.

LEE, H.Y., 1975. Conodonten aus dem unteren und mittleren Ordovizium von Nordkorea. *Palaeontographica Abteilung A 150*, 161-186.

LEE, H.Y., 1976. Conodonts from the Maggol- and Jeongseon Formations (Ordovician), Kangweon-Do, South Korea. *Journal of the Geological Society of Korea 12*, 151-181.

LESLIE, S.A. 2000. Mohawkian (Upper Ordovician) conodonts of eastern North America and Baltoscandia. *Journal of Paleontology 74*, 1122-1147.

LINDSTRÖM, M., 1955. Conodonts from the lowermost Ordovician strata of south-central Sweden. *Geologiska Föreningens i Stockholm Förhandlingar 76*, 517-604.

LINDSTRÖM, M., 1971. Lower Ordovician conodonts of Europe. *Geological Society of America, Memoir 127*, 21-61.

LÖFGREN, A., 1978. Arenigian and Llanvirnian conodonts from Jämtland, northern Sweden. *Fossils and Strata 13*, 1-129.

LÖFGREN, A., 1993. Arenig conodont successions from central Sweden. *Geologiska Föreningens i Stockholm Förhandlingar 115*, 193–207.

LÖFGREN, A., 1994. Arenig (Lower Ordovician) conodonts and biozonation in the eastern Siljan District, central Sweden. *Journal of Paleontology 68*, 1350–1368.

LÖFGREN, A., 1995. The probable origin of the Ordovician conodont "*Cordylodus*" *horridus*. *Geobios 28*, 371-377.

LÖFGREN, A., 1997. Reinterpretation of the Lower Ordovician conodont apparatus *Paroistodus*. *Palaeontology 40*, 913-929.

LÖFGREN, A., 2003. Conodont faunas with *Lenodus variabilis* in the upper Arenigian to lower Llanvirnian of Sweden. *Acta Palaeontologica Polonica 48*, 417-436.

LÖFGREN, A., 2004. The conodont fauna in the Middle

Ordovician *Eoplacognathus pseudoplanus* Zone of Baltoscandia. *Geological Magazine 141*, 505-524.

Löfgren, A., 2006. An *Oistodus venustus*-like conodont species from the Middle Ordovician of Baltoscandia. *Paläontologische Zeitschrift 80*, 12–21.

Löfgren, A. & Tolmacheva, T.J., 2003. Taxonomy and distribution of the Ordovician conodont *Drepanodus arcuatus* Pander, 1856, and related species. *Paläontologische Zeitschrift 77*, 203–221.

Mellgren, J. & Eriksson, M.E., 2006. A model of reconstruction for the oral apparatus of the Ordovician conodont genus *Protopanderodus* Lindström, 1971. *Transactions of the Royal Society of Edinburgh: Earth Sciences 97*, 97–112.

Nowlan, G.S. & Thurlow, J.G., 1984. Middle Ordovician conodonts from the Buchans Group, central Newfoundland, and their significance for regional stratigraphy of the Central Volcanic Belt. *Canadian Journal of Earth Sciences 21*, 284-296.

Pander, C.H., 1856. *Monographie der fossilen Fische des Silurischen Systems der Russisch-Baltischen Gouvernements*. Akademie der Wissenschaften, St. Petersburg, 91 p.

Percival, I.G. & Zhen Y.Y., 2007. Darriwilian conodonts of Eastern Australia: biostratigraphy and biogeographic distribution. *Acta Palaeontologica Sinica 46 (Supplement)*, 387-392.

Pyle, L.J., Barnes, C.R. & Ji Z.L., 2003. Conodont fauna and biostratigraphy of the Outram, Skoki, and Owen Creek formations (Lower to Middle Ordovician), Wilcox Pass, Alberta, Canada. *Journal of Paleontology 77*, 958-976.

Rasmussen, J.A., 2001. Conodont biostratigraphy and taxonomy of the Ordovician shelf margin deposits in the Scandinavian Caledonides. *Fossils and Strata 48*, 1-180.

Rattenbury, M., Cooper, R.A. & Johnston, M.R., 1998. *Geology of the Nelson area, 1:250 000 geological map 9.* Institute of Geological and Nuclear Sciences Lower Hutt. 1 sheet + 67 p.

Sergeeva, S.P., 1963. Conodonts from the Lower Ordovician of the Leningrad region. *Paleontologicheskiy Zhurnal 2*, 93-108.

Serpagli, E., 1967. I conodonti dell'Ordoviciano superiore (Ashgiliano) delle Alpi Carniche. *Bolletino della Societá Paleontologica Italiana 6*, 3-111.

Serpagli, E., 1974. Lower Ordovician conodonts from Precordilleran Argentina (Province of San Juan). *Bollettino della Società Paleontologica Italiana 13*, 17-98.

Simes, J.E., 1980. Age of the Arthur Marble: conodont evidence from Mount Owen, northwest Nelson. *New Zealand Journal of Geology and Geophysics 23*, 529-532.

Stait, K. & Druce, E.C., 1993. Conodonts from the Lower Ordovician Coolibah Formation, Georgina Basin, central Australia. *BMR Journal of Australian Geology & Geophysics 13*, 293-322.

Stauffer, C.R., 1935. Conodonts of the Glenwood beds. *Geological Society of America Bulletin 46*, 125-168.

Stouge, S., 1984. Conodonts of the Middle Ordovician Table Head Formation, western Newfoundland. *Fossils and Strata 16*, 1-145.

Stouge, S. & Bagnoli, G., 1988. Early Ordovician conodonts from Cow Head Peninsula, western Newfoundland. *Palaeontographica Italica 75*, 89-179.

Stouge, S. & Bagnoli, G., 1990. Lower Ordovician (Volkhovian-Kundan) conodonts from Hagudden northern Öland, Sweden. *Palaeontographia Italica 77*, 1-54.

Sweet, W.C., 1988. *The Conodonta: Morphology, Taxonomy, Paleoecology, and Evolutionary History of a Long-Extinct Animal Phylum*. Clarendon Press, Oxford, 212 p.

Sweet, W.C. & Bergström, S.M., 1962. Conodonts from the Pratt Ferry Formation (Middle Ordovician) of Alabama. *Journal of Paleontology 36*, 1214-1252.

Tolmacheva, T.J., 2006. Apparatus of the conodont *Scolopodus striatus* Pander, 1856 and a re-evaluation of Pander's species of *Scolopodus*. *Acta Palaeontologica Polonica 51*, 247–260.

Tolmacheva, T.J. & Fedorov, P., 2001. The Ordovician Billingen/Volkhov boundary interval (Arenig) at Lava River, northwestern Russia. *Norsk Geologisk Tidsskrift 81*, 161–168.

Viira, V., 1974. *Konodonty ordovika Pribaltiki*. Valgus, Tallinn, 142 p.

Viira, V., Löfgren, A., Mägi, S. & Wickström, J., 2001. An Early to Middle Ordovician succession of conodont faunas at Mäekalda, northern Estonia. *Geological Magazine 138*, 699–718.

Wamel, W.A. van, 1974. Conodont biostratigraphy of the Upper Cambrian and Lower Ordovician of north-western Öland, south-eastern Sweden. *Utrecht Micropalaeontological Bulletin 10*, 1-125.

Wang Z.H. & Luo K.Q., 1984. Late Cambrian and Ordovician conodonts from the marginal areas of the Ordos Platform, China. *Bulletin of Nanjing Institute of Geology and Palaeontology 8*, 237-304.

Watson, S.T., 1988. Ordovician conodonts from the Canning Basin (W. Australia). *Palaeontographica Abteilung A 203*, 91-147.

Webby, B.D., Paris, F., Droser, M.L. & Percival, I.G. (eds), 2004. *The Great Ordovician biodiversification event*. Columbia University Press, New York, 484 p.

Wright, A.J., 1968. Ordovician conodonts from New Zealand. *Nature 218*, 664-665.

Wright, A.J., Cooper, R.A. & Simes, J.E., 1994. Cambrian and Ordovician faunas and stratigraphy, Mt Patriarch, New Zealand. *New Zealand Journal of Geology and Geophysics 37*, 437-476.

Zhang J.H., 1998. Conodonts from the Guniutan Formation (Llanvirnian) in Hubei and Hunan Provinces, south-central China. *Stockholm Contributions in Geology 46*, 1-161.

Zhang S.X. & Barnes, C.R., 2002. A new Llandovery (Early Silurian) conodont biozonation and conodonts from the Becscie, Merrimack, and Gun River Formations, Anticosti Island, Québec. *Journal of Paleontology 76 (Supplement to No. 2)*, 1-46.

Zhao Z.X., Zhang G.Z. & Xiao J.N., 2000. *Palaeozoic stratigraphy and conodonts in Xinjiang*. Petroleum Industry Press, Beijing, 340 p.

Zhen Y.Y. & Percival, I.G., 2004a. Middle Ordovician (Darriwilian) conodonts from allochthonous limestones in the Oakdale Formation of central New South Wales, Australia. *Alcheringa 28*, 77-111.

Zhen Y.Y. & Percival, I.G., 2004b. Middle Ordovician (Darriwilian) conodonts from the Weemalla Formation, south of Orange, New South Wales. *Memoirs of the Association of Australasian Palaeontologists 30*, 153-178.

Zhen Y.Y., Percival, I.G. & Liu, J.B., 2006. *Triangulodus* (Conodonta) from the Early Ordovician Honghuayuan Formation of Guizhou, South China. *Alcheringa 30*, 191-212.

Zhen Y.Y., Percival, I.G., Löfgren, A. & Liu, J.B., 2007. Drepanoistodontid conodonts from the Early Ordovician Honghuayuan Formation of Guizhou, South China. *Acta Micropalaeontologica Sinica 24*, 125-148.

Zhen Y.Y., Percival, I.G. & Webby, B.D., 2003. Early Ordovician conodonts from western New South Wales, Australia. *Records of the Australian Museum 55*, 169-220.

Zhen Y.Y., Percival, I.G. & Webby, B.D., 2004a. Early Ordovician (Bendigonian) conodonts from central New South Wales, Australia. *Courier Forschungsinstitut Senckenberg 245*, 39-73.

Zhen Y.Y., Percival, I.G. & Webby, B.D., 2004b. Conodont faunas from the Mid to Late Ordovician boundary interval of the Wahringa Limestone Member (Fairbridge Volcanics), central New South Wales. *Proceedings of the Linnean Society of New South Wales 125*, 141-164.

Zhen Y.Y. & Pickett, J.W., 2008. Ordovician (Early Darriwilian) conodonts and sponges from west of Parkes, central New South Wales. *Proceedings of the Linnean Society of New South Wales 129*, 57-82.

Zhen Y.Y., Zhang, Y.D. & Percival, I.G., 2009. Early Sandbian (Late Ordovician) conodonts from the Yenwashan Formation, western Zhejiang, South China. *Alcheringa 33*, 133-161.

Ziegler, W. (ed.), 1974. *Catalogue of conodonts*. Schweizerbartsche, Stuttgart, Volume 1, 504 p.